KfK 4019
Juni 1986

Application of Different Methods of Neutron Activation Analysis to the Determination of Trace Elements in Rock Samples

R. Zaghloul, E. Gantner, M. Mostafa, H. J. Ache
Institut für Radiochemie

Kernforschungszentrum Karlsruhe

KERNFORSCHUNGSZENTRUM KARLSRUHE

Institut für Radiochemie

KfK 4019

Application of Different Methods of Neutron Activation Analysis to the Determination of Trace Elements in Rock Samples

R. Zaghloul*, E. Gantner, M. Mostafa and H.J. Ache

Kernforschungszentrum Karlsruhe GmbH, Karlsruhe

* Visiting scientist from Atomic Energy Authority, Cairo, Egypt

Kernforschungszentrum Karlsruhe GmbH
Postfach 3640, 7500 Karlsruhe 1

ISSN 0303-4003

Abstract

In this report three different methods of neutron activation analysis applied to the determination of up to 20 trace elements in Egyptian rock samples and the results obtained are discussed. In Part I a physical approach is described for instrumental multielement activation analysis with whole neutron spectrum (without Cd-cover) using the monostandard (single comparator) method. To test the capabilities of this method, 15 samples representing different Egyptian granite rocks were analyzed. As many as 21 trace elements beside Fe, K and Na were determined. Calculation of the experimental data has been done using the "Gamma-Monostandard Analysis" program with the Commodore Computer at the Institute of Radiochemistry at Garching near München. The accuracy of the method for nondestructive multi-element analysis agrees within 3 % with the relative method using multielement standards.

In Part II a method is described for epithermal neutron activation analysis of 20 elements in granite rock samples using only one standard. Gold has been used as a single comparator due to its relatively high resonance integral value (I_o = 400) and in addition, it is preferable on Co in order to obtain a large epithermal activation in a short irradiation. The method of calculation is simple and rapid and can be done using small calculator. Epithermal activation is able to overcome the difficulty arising from changing irradiation position as well as increasing the number of determinable elements by eliminating the interference from undesired isotopes which have relatively high thermal cross-section values (σ_o), when reactor neutron flux are used. The coupling of the epithermal activation with the monostandard method has the advantage of using a small Cd-cover which overcomes most of the difficulties which arise in the relative method using large volume cadmium filters.

In Part III experiments are described in which a neutron capture gamma-ray spectroscopy facility assembled at the Institute of Radiochemistry, KfK (for analytical purposes) using Cf^{252} neutron source of strength $\sim$ 6 x 10^7 n/sec, has been used to check its applicability and sensitivity for quantitative analyses of ores. The analysis of Sm, Gd and Mn in phosphate and monazite rock samples has been carried out. The results from this study show a variation of about 25 % from the values determined by RNAA method. This discrepancy could be mainly due to the low signal-to-background ratio observed which is caused by the i) scattering of the source gamma-rays by the target and ii) interference from the 2223.1 keV neutron capture hydrogen gamma-rays produced by the moderated materials and from their compton scattering in the detector.

To overcome these difficulties we suggest to introduce a 2.5 cm thick polyethylene sheet between the detector Li^6-cap shielding and the target as well as to increase the detection solid-angle. Also the strength of the Cf^{252} neutron source should be increased by an order of magnitude and the neutron beam should be collimated to obtain the optimal thermal neutron flux with low level of Cf^{252} gamma-rays. This can be fulfilled by setting-up between the neutron source and the target a conical collimator from polyethylene with a thickness of 10 cm containing a 1 cm thick lead sheet.

Anwendung verschiedener Methoden der Neutronenaktivierungsanalyse auf die Bestimmung von Spurenelementen in Gesteinsproben

Zusammenfassung

In dieser Arbeit werden drei verschiedene Methoden der Neutronenaktivierungsanalyse, die auf die Bestimmung von bis zu 20 Spurenelementen in ägyptischen Gesteinsproben angewandt wurden, zusammen mit den dabei erhaltenen Ergebnissen diskutiert.

In Teil I wird eine physikalische Methode zur instrumentellen Multielement-Aktivierungsanalyse mit Reaktorneutronen (ohne Cd-Hülle) unter Verwendung eines einzelnen Standards ("Single Comparator Method") beschrieben. Um die Eignung der Methode zu testen, wurden 15 Proben aus verschiedenen ägyptischen Graniten analysiert und auf diesem Weg neben Fe, K und Na insgesamt 21 Spurenelemente bestimmt. Die Berechnungen wurden unter Verwendung der Meßdaten mit dem "Gamma-Monostandard Analysis"-Programm (Commodore Rechner) am Institut für Radiochemie in Garching bei München durchgeführt. Die Genauigkeit der Methode ist innerhalb ca. 3 % vergleichbar mit der der relativen Methode, bei der Multielementstandards verwendet werden.

In Teil II wird eine Methode zur epithermischen Neutronenaktivierungsanalyse von 20 Elementen in Granitproben unter Verwendung eines einzigen Standards beschrieben. Als Einzelstandard wurde Gold wegen seines hohen Resonanzintegrals (I_o = 400) verwendet, das außerdem gegenüber Kobalt auch bei kurzen Bestrahlungszeiten durch epithermische Neutronen merklich aktiviert wird. Die zur Auswertung erforderlichen Berechnungen sind einfach und lassen sich mit einem kleinen Tischrechner schnell durchführen. Bei der epithermischen Aktivierung entfallen die Schwierigkeiten, die sich aufgrund unterschiedlicher Bestrahlungspositionen ergeben. Außerdem erhöht sich

die Zahl der bestimmbaren Elemente, da Störungen durch Isotope mit hohem thermischen Wirkungsquerschnitt (σ_0) ausgeschaltet werden. Die Verbindung von epithermischer Aktivierung mit der Einstandardmethode hat ferner den Vorteil, daß nur eine kleinvolumige Cd-Umhüllung benötigt wird. Damit entfallen die meisten Schwierigkeiten, die sich bei der relativen Methode mit großvolumigen Cd-Filtern ergeben.

In Teil III werden Experimente zur Untersuchung der Eignung und Empfindlichkeit der im Institut für Radiochemie / KfK aufgebauten, mit einer Cf-252-Quelle (Quellstärke ca. 6 x 10^7 n/sec) ausgestatteten Anordnung für die Neutroneneinfangs-γ-Spektroskopie für die quantitative Mineralanalyse am Beispiel der Bestimmung von Sm, Gd und Mn in Phosphat- und Monazitproben beschrieben. Die dabei erhaltenen Ergebnisse weichen um bis zu 25 % von den durch Reaktorneutronenaktivierung gefundenen Werten ab. Diese Abweichung dürfte hauptsächlich auf das ungünstige Signal-Untergrund-Verhältnis zurückzuführen sein, dessen Ursachen i) die Streuung der von der Quelle ausgehenden γ-Strahlung an der Probe und ii) die Störung durch die 2223.1 keV γ-Quanten sind, die mit hoher Intensität durch Neutroneneinfang an den Wasserstoffatomen des Moderatormaterials entstehen und im Detektor vorwiegend durch Comptonstreuung nachgewiesen werden.

Zur Vermeidung dieser Schwierigkeiten schlagen wir vor, eine 2,5 cm dicke Polyacethylenscheibe zwischen Li^6-Detektorabdeckung und der Probe anzubringen und die Meßgeometrie zu verbessern. Außerdem sollte die Stärke der Neutronenquelle um etwa eine Größenordnung erhöht und der Neutronenstrahl kollimiert werden, um den maximalen thermischen Neutronenfluß mit geringem Anteil an Quellen-γ-Strahlung am Probenort zu erhalten. Hierfür eignet sich ein 10 cm dicker konischer Kollimator aus Polyacethylen zwischen Neutronenquelle und Target, der mit 1 cm dickem Blei beschichtet ist.

I. Neutron Activation Analysis without Multielement Standards

1. Introduction

Almost, neutron activation analysis (NAA) has been used as a relative method in which the sample and a standard containing known amounts of the elements of interest are irradiated simultaneously, followed by measurement of their activities under identical conditions. Comparison of the activities of the sample with those of standard of known concentration allows a simple calculation of the concentration of an element in the sample.

The approach has worked well when only one or a few elements had to be determined; however, problems arise when a great number of elements in one sample has to be determined, the treatment of the standards in the way of preparation, dissolution, counting and so on is very cumbersome and time-consuming, beside the difficulty arising due to irradiate a large number of standards and samples together in one capsule. These reasons and the advent of high resolution Ge(Li) detectors, multichannel pulse height analyzers, and computerized data processing led many authors (1-18) to use monostandard (also called single comparator) method for multielement determination. In this method the specific photopeak activities of the isotopes investigated are compared with the specific photopeak acitivity of a comparator, both measured in well-defined experimental conditions. These ratios are defined as K-values. The method provides the precision and accuracy which may overcome the relative method. The accuracy of determining each element depends obviously on uncertainties of the nuclear data involved and hence differs from element to element. The nuclear data determined during the last ten years are accurate enough to be applied for the monostandard method.

This work presents a discussion on the physical significance of the monostandard method relevant to analytical purposes. Results on the application of this approach to the analysis of 24 elements in 15 different granite rock samples from Egypt are outlined.

2. Physical treatment of monostandard method

For any reaction whose cross section varies inversely as the neutron velocity "obeys the 1/V law", the effective value for any neutron spectrum is just the 2200 m/sec cross section normally tabulated. For this law the reaction rate is proportional to the neutron density and is independent of the neutron spectrum. An alternative statement of this convention is that the effective cross section $\hat{\sigma}$ of a nuclide is a reaction parameter which is not constant but a function of the characteristics of the neutron energy spectrum, and is defined by equating the reaction rate R per atom present in the flux nV_o:

$$R = nV_o \qquad (1)$$

where n is the neutron density, including both thermal and epithermal neutrons, and V_o equal to 2.2×10^5 cm/sec (2200 m/sec).

When the cross section departs from the 1/V law, a simple relation can be obtained giving $\hat{\sigma}$ for the spectrum of a well-moderated thermal-neutron reactor.

The neutron spectrum is assumed to be the sum of the components, an epithermal dE/E flux distribution cut-off at a suitable lower limit of energy μKT and a Maxwellian distribution corresponding to T°K, where $\mu \cong 5$ for many research reactors and K is the Boltzmann constant. The two components overlap in energy, since no cut-off is imposed on the Maxwellian component. By introducing the relative strength $\gamma\sqrt{T/T_o}$ of the epithermal dE/E component, the reaction rate R in eq. (1) can be put in another form according to Westcott (19-21) assumption as

$$R = nV_o \hat{\sigma} = nV_o \sigma_o (g + \gamma\sqrt{T/T_o}\, S_o) \qquad (2)$$

Therefore

$$\hat{\sigma} = \sigma_o (g + \gamma\sqrt{T/T_o}\, S_o)$$

where σ_o is the cross-section of neutrons of velocity V_o = 2200 m/sec and of energy KT_o, T_o = 293.6 °K (20.44 °C), g & S_o are functions of the temperature T depending on the departure of the cross-section law from the 1/V form (for a 1/V law, g = 1 & S_o = 0). According to Halperin et al. (22) the reaction rate R is given by

$$R = nV_o \hat{\sigma} = \phi_{th} (g\,\sigma_o + (\phi_{ep}/\phi_{th})\, I'_o) \qquad (3)$$

or

$$R = nV_o \hat{\sigma} = \phi_{th} (\sigma_{th} + (\phi_{ep}/\phi_{th})\, I_o) \qquad (4)$$

Since nV_o is the thermal neutron flux ϕ_{th}, so that eqs. (2) and (3) yield the relation (23)

$$\phi_{ep}/\phi_{th} = (2/\sqrt{\pi})\, \gamma\sqrt{T/T_o} \qquad (5)$$

and

$$\sigma_{th} = g\,\sigma_o + (2/\sqrt{\pi})\, \gamma\sqrt{T/T_o}\, (I'_o - I_o) \qquad (6)$$

where $\tilde{\sigma}_{th}$ = subcadmium (< E_c) thermal cross-section,

I_o = epicadmium (> E_c) resonance integral with 1/V tail

so $$I_o = \int_{E_c}^{\infty} (E)\, dE/E \qquad (7)$$

Φ_{th} = thermal neutron flux (subcadmium flux)

Φ_{ep} = epithermal neutron flux (epicadmium flux)

I'_o = resonance integral with an effective lower energy limit μKT and with a 1/V-term excluded

so $$I'_o = \int_{\mu KT}^{\infty} \left(\tilde{\sigma}(E) - g\, \tilde{\sigma}_o \sqrt{E_o/E} \right) dE/E \qquad (8)$$

The common method followed to determined I_o for a nuclide is the activation of the target under a Cd-filter and hence the difference $I'_o - I_o$ in eq (6) is given (24) by

$$I'_o - I_o = \int_{\mu KT}^{E_c} \left[\tilde{\sigma}(e) - g\, \tilde{\sigma}_o \sqrt{E_o/E} \right] dE/E - \int_{E_c}^{\infty} g\, \tilde{\sigma}_o \sqrt{E_o/E}\, dE/E$$

$$= \Delta I'_o - I_o \text{ (1/V-tailing)} \qquad (9)$$

From eqs (6) and (9) one can get

$$\tilde{\sigma}_{th} = g\, \tilde{\sigma}_o + (2/\sqrt{\pi})\, r \sqrt{T/T_o} \left[\Delta I'_o - I_o \text{ (1/V-tailing)} \right] \qquad (10)$$

and eq (9) yields

$$I_o = I'_o + 2\, g\, \tilde{\sigma}_o \sqrt{E_o/E_c}, \quad (\Delta I'_o \cong 0) \qquad (11)$$

for a target nuclide has resonance peaks far above 0.5 eV (E_c). In the literature (24,25), $\tilde{\sigma}_o$ and I'_o (or I_o) are given, whereas $\tilde{\sigma}_{th}$ must be evaluated in accordance with eq. (10), if the reaction rate will be calculated by eq. (4). The g(T) values for a number of nuclides which have $g(T) \neq 1$, are given as a function of the neutron temperature (26,27). A compilation of resonance integrals I'_o or I_o for all nuclides from hydrogen to fermium is available in the literature (28).

The effective cross section $\hat{\sigma}$ for a given irradiation position is then available when the flux index $r\sqrt{T/T_o}$ is known. $r\sqrt{T/T_o}$ is the epithermal index which denotes the strength of the epithermal flux and it is constant for each irradiation site with a steady operation of the reactor, and can be determined by measuring the Cd-ratio C_R of a monitor nuclide using the relation (23)

$$r\sqrt{T/T_o} = g/\left[(C_R - 1)\, S_o + 4\, C_R \sqrt{E_o/\pi E_c}\right] \qquad (12)$$

where $r\sqrt{T/T_o}$ equals zero for a pure thermal neutron flux, S_o is a parameter which represents the ratio of the resonance integral and thermal cross-section, such that (28)

$$S_o = \frac{2}{\sqrt{\pi}\,\sigma_o} \int_{\mu KT}^{\infty} \left[(E) - g(T)\, \sigma_o \sqrt{E_o/E}\right] dE/E = 2/\sqrt{\pi}\,(I'_o/\sigma_o) \qquad (13)$$

The epithermal index $r\sqrt{T/T_o}$ for a given irradiation position can be determined either with eq. (12) by measuring the Cd-ratio of one monitor or from the irradiation without Cd-cover of two different monitor nuclides, one must be sensitive to thermal neutrons and the other to epithermal (resonance) neutrons. From the simultaneous irradiation of the two monitors, the epithermal index for a given position is evaluated (28) by

$$r\sqrt{T/T_o} = (g_1\, \sigma_{o1} - g_2\, \sigma_{o2}\, R)/(S_{o2}\, \sigma_{o2}\, R - S_{o1}\, \sigma_{o1}) \qquad (14)$$

where the suffixes 1 and 2 distinguish the two nuclides and R represents $\hat{\sigma}_1/\hat{\sigma}_2$, which can be determined by measuring the relative specific activities of the two monitor nuclides (29).

Either monitors can be irradiated with samples and used also as the monostandard. The first method (eq. 12) requires the knowledge of a cut-off energy E_c, which is not easy to determine, since it is a function of the thickness of a Cd-filter, its shape, neutron energy and angle of incidence. For this reason, the second method (eq. 14) is preferred. The multicomparator technique described in the literature (12,14,15) is the same procedure given by eq. (14). When $r\sqrt{T/T_o}$ is known, $\hat{\sigma}$ for all nuclides of interest can be computed by eq. 2 and then the application of monostandard method is possible for any nuclide observed in gamma-spectra using the following equation given by Kim (23)

$$M_i = M^* \frac{A_i}{A^*} \left(\frac{R_s R_d}{C_1 C_2 C_3 C_4} \right) \qquad (15)$$

or

$$M_i = M^* \frac{A_i}{A^*} R_s R_d K \qquad (16)$$

where

$$C_1 = \frac{f_i M^*}{f^* M}, \quad C_2 = \frac{b_i}{b^*}, \quad C_3 = \frac{\epsilon_i}{\epsilon^*}, \quad C_4 = \frac{\hat{\sigma}_i}{\hat{\sigma}^*}$$

$$R_s = (1 - e^{-\lambda^* t_1}) / (1 - e^{-\lambda_i t_1}), \quad R_d = e^{-\lambda^* t_2} / e^{-\lambda_i t_2}$$

$\hat{\sigma}$ - Effective activation cross section derived from the reaction rate, $R = nV_o\hat{\sigma}$ (n : total neutron density, V_o = 2200 m/sec);

ϵ - detection efficiency of a detector for a particular gamma-ray energy;

b - absolute gamma-intensity from the total disintegration corrected for the electron conversion rate;

f - fractional isotopic abundance of the nuclide;

M - atomic weight of the nuclide per mole;

λ - decay constant;

t_1 - irradiation time;

t_2 - decay time

whereas C_1 and C_2 are absolute constants, C_3 and C_4 are apparant constants with respect to a definite set of experimental conditions and hence K in eq. (16) is an apparent constant. C_3 and C_4 vary, respectively with the properties of the detector used as well as the sample geometry, and with an energy spectrum of the neutron flux at an irradiation site. Since the experimental conditions of the used set is fixed, C_3 is determined for the particular sample geometry and the given detector, whereas C_4 remains constant with respect to the flux index and the monitor.

3. Experimental

3.1 Irradiation

All irradiations were performed for a period of exactly 1 hour in the Triga II reactor of the Institute of Nuclear Medicine of DKFZ, Heidelberg. The reactor was operating at a constant power of 250 KW. The thermal and epithermal neutron flux of the irradiation site were determined by the usual Co and Au flux monitors, irradiated with and without Cd-cover. The flux index r T/T_o for the irradiation condition is evaluated with the two different methods using eqs. (12) and (14). About 100 mg of each sample from the 15 different granite rock samples brought from Egypt were weighed and sealed in cleaned small polyethelene vials for such short irradiations. To prevent the vials from sticking and neutron flux depression and to obtain better heat dissipation and homogenity in neutron flux distribution around the sample they have been distributed into 3 groups, each with their independent monostandards (Co and Au for flux monitor) and wrapped together in aluminium foil. These were then put into aluminium can for irradiation.

3.2 Activity measurements

Gamma-spectra were measured with a Ge(Li) detector of volume 35 CC connected to a 4096 channel PHA which is coupled to an PDP-11/34 computer. The energy resolution of the detector is 1.9 keV FWHM for the 1.33 MeV peak of Co^{60}. The detector is well shielded by keeping it inside a lead-brick chamber of 5 cm thick and lined with thin copper sheet to prevent the backscattering of the gamma-rays. The energy calibration and detection efficiency were determined by using standard sources of Co^{57}, Co^{60}, Y^{88}, Cs^{137}, Am^{241} and Hg^{203}. The efficiency curves were obtained for energy range up to 2000 keV for geometries of 10 cm and 40 cm from the detector. For the first geometry, the efficiency range is from 3.355×10^{-4} to 1.111×10^{-2}. The equation used by the CAMBERRA "CALIB" program for the efficiency calibration are:

In case of the first geometry for low energy coefficients

$$\log (Eff) = -50.9843 + 22.0357 \log (E) - 3.2464 \log (E)^2 + 0.1345 \log (E)^3$$

For high energy coefficients

$$\log (Eff) = 1.2444 - 1.4526 \log (E) + 0.03523 \log (E)^2$$

and cross-over energy = 279.0 keV.

For the second geometry, the efficiency range is from 4.54×10^{-5} to 9.119×10^{-4}, and the efficiency equations are:

For low energy coefficients

$$\log (Eff) = -63.4881 + 29.1507 \log (E) - 4.8808 \log (E)^2 + 0.2574 \log (E)^3$$

for high energy coefficients

$$\log (Eff) = -2.5835 - 0.9973 \log (E) + 0.00161 \log (E)^2$$

and cross-over energy = 279.0 keV.

The measurements of the γ-ray spectra of the activated rock samples were started 4 days after the end of irradiation to allow the induced activities from the short-lived isotopes produced within the sample to diminish to the point where it no longer interfered. The measurements were performed in two series. In the first measurement, taken after 4-7 days, γ-activity from the nuclides As^{76}, Ga^{72}, K^{42}, La^{140}, Sm^{153}, Sb^{122}, W^{187} and Np^{239} was registered. The second series of measurements was performed after 20-23 days in which the rest of the activities in question were recorded. For each sample measurement time was 1 hour and the dead time did not exceed 3-4 %. The 15 different granite rock samples have been divided into 2 groups as given by tables (3-a) and (3-b). The γ-spectra of the AD-103 granite samples from the first group are depicted in figs. 3 and 4 measured after 5 days and 22 days from the end of irradiation, respectively, while figs. 5 and 6 show the γ-spectra for a granite sample (As-3) from the second group (table 3-b) for 6 days and 21 days decay periods, respectively.

4. Results and discussions

A set of absolute radioactive standards containing Co^{57}, Co^{60}, Y^{88}, Cs^{137}, Am^{241} and Hg^{203} is used to calibrate the Ge(Li) detector for two detector-source distances 10 and 40 cm. Figs. 1 and 2 show the efficiency calibration at the 10 cm and 40 cm geometry curves, respectively, while the efficiency values determined experimentally for the γ-energies involved are listed in table 1 (a and b) for both geometries. The technique followed in the calibration is the one used by Ricci (30) which provides an absolute calibration of the detector so that it can be considered that eq. (15) is applied with C_3 on the absolute basis and C_4 evaluated by the help of a chosen flux monitor.

The induced γ-activity of the irradiated rock samples for 1 hour at whole reactor neutron flux, ϕ_t of 5.02 x 10^{12} n/cm² · sec, was measured at two decay periods chosen according to the half-lives of the 24 present isotopes. During the first period after 4 days from the end of irradiation, elements As, Au, K, La, Na, Sb, Sm, W, Yb and U could be determined, and the elements Ce, Co, Cr, Cs, Eu, Fe, Hf, Lu, Rb, Sc, Sn, Ta, Tb and Th after 20 days have been recorded. The measured γ-spectra taken through these two periods are shown in figs. 3 to 6. The quantitative analysis was carried out for some radioisotopes using the most favorable peaks (1099.3 & 1291.9 keV for Fe-59, 889.4 & 1120.5 keV for Sc-46 and 1188.9 & 1221.3 keV for Ta-182) which usually are the highest energy peaks and normally have less interferences than lower energy peaks, due to the Compton effect. In all other cases the elements were determined by their most prominent peaks, free of interference and with lower statistical errors. Table 2 shows the selected γ-energies, which give the most accurate results. The nuclear properties of the elements determined by monostandard activation analysis technique are compiled (23,28) in Table 2. The cross-sections given in the table are valid for eq. (2). Wherever eq. (4) is used for the evaluation of effective cross-sections $_{th}$ & I_o, the cross-sections given in Table 2 (σ_o & I'_o) must be used after appropriate corrections according to eqs. (10) and (11).

Monostandard method is used mainly for whole reactor (thermal and epithermal) and epithermal (under cadmium) neutron activation. In Part I, the monostandard approach is introduced for the whole reactor neutron activation analysis, while for epithermal is handled in Part II of this report. Therefore, the flux index $r\sqrt{T/T_o}$ for the irradiation position at the reactor and the use of a chosen monostandard element are essential. In principle any element can be used as a monostandard if the nuclear data of a chosen nuclide are well known. Co and Au are found to be the convenient candidates. Both nuclides Au^{197} and Co^{59} are 100 % in the isotopic abundance and their nuclear data are accurately known (28). The large difference in the cross-section parameters S_o of Au^{197} (= 17.28) and Co^{59} (= 1.78) facilitates the determination of $r\sqrt{T/T_o}$ for any irradiated condition without using a Cd-filter. $r\sqrt{T/T_o}$ has been estimated by the two methods described in this work using eqs (12) and (14), leading to 0.011 and 0.012, respectively, and to a value of 84 for the thermal-to-epithermal (ϕ_{th}/ϕ_{ep}) neutron flux ratio (ϕ_{th} = 4.96 x 10^{12} n/cm²·sec and ϕ_{ep} = 5.9 x 10^{10} n/cm² sec). As pointed out before, the value determined by the Cd-ratio method (eq. 12) is found to be lower by about 8 % than the value obtained from the other method (eq. 14). This proves that the double monitors technique for determining the flux index $r\sqrt{T/T_o}$ is more promising.

The net γ -peak areas were evaluated with the PDP-11/34 digital computer connected with the measuring system, utilizing the program "SPEKTRAN-F". This program (31) automatically searches for significant peaks from the digital data of the spectra stored on disk and calculates the net areas of the peaks by subtraction from an artificial baseline under der peaks, which represents the natural background and the Compton Continua from the more energetic peaks on the spectra. The monostandard analysis of the net peak area for the 15 granite rock samples have been processed using the "Gamma-Monostandard Analysis" program run by the Commodore Computer at the Institute of Radiochemistry at Garching near München. The results obtained for the concentration of Fe, K, Na and of 21 trace elements in 15 samples of different Egyptian granite rocks are indicated in Table (3-a) and (3-b), expressed in parts per million unless otherwise indicated. This table shows that the most abundant among a total of 24 analyzed elements are the trace elements Hf, La, Lu, Sc, Sm and Yb besides Fe, K, Na and Th which could be determined with acceptable precision. Sc has the most favorable properties for this method of analysis in rocks. It has 100 % abundance of its single stable nuclide beside its 100 % branching ratio of the measured γ-lines 889.4 keV and 1120.5 keV as given in Table 2. The convenient half-life of 83.9 days and relatively high cross-section as well as the sensitivity and precision of determining this element by RNAA are quite favorable. The interference due to uranium fission for elements Ce and La has been quantitatively considered. The concentration values of the elements recorded in Table 3 (a & b) have errors with mean values ranging from 10-15 %. The most significant contribution comes from the uncertainties in the determination of the spectral index ($\gamma\sqrt{T/T_o}$) and the dissimilarity of samples and standard used. The one used was Co in sponge form, while the best convenient monostandard commonly utilised in this technique is the commercially available Co-Al alloy wire with 0.1 wt % Co. On the other hand, the method excludes automatically the errors possibly resulting from treatments of individual standards. In general the observed element contents are within the statistical errors of the measurements of the photopeak areas. However, the accuracy of the monostandard method adopted in the analysis of the granite rock samples is as good as that of the conventional relative method.

5. Conclusions

From the results of this work it appears that a combination of the two procedures (RNAA) and ENAA) coupled with the monostandard method might be necessary for the analysis of the largest number of elements in a given sample. However, each procedure may be considered more suitable for the analysis of certain elements in

the sample depending on their nuclear properties, matrix composition and concentration level as well as the irradiation conditions. The main criteria for the choice of one of the two procedures are summarized as follows.

The procedure of RNAA coupled with monostandard method is suitable for elements with relatively high thermal cross-sections (σ_o) compared to the resonance integrals (I_o), such as Ca, Ce, Cr, Eu, Fe, Lu and Se. The advantage of this technique is its higher sensitivity for these elements but at the same time its disadvantage is due to the interference from the epithermal activated elements present in the same sample, due to the contribution of the two neutron components (thermal and epithermal) in the activation process, while the second technique using ENAA is more favorable for elements having relatively high resonance integrals (I_o), such as Ba, Br, Co, Cs, Hf, Rb, Sb, Se, Sm, Sr, Ta, Tb, Th, U and Zr. In this way not only the number of determinable elements is increased, but also the difficulty due to changing irradiation position is overcome, the sensitivity and accuracy are improved for many trace elements. Besides that the technique can be effectively used on routine basis for the analysis of a large number of samples encountered in the prospection and geochemical investigation. These reasons led the authors to handle this technique in more details.

II. Epithermal Neutron Activation Analysis Using the Monostandard Method

1. Introduction

Neutron activation analysis by the relative method is still the direct, simple and most accurate method when a certain element or a limited number of elements are to be determined. However, in the case of simultaneous determination of a large number of elements the relative method requires preparation and counting of a standard for each element to be determined. These processes are time-consuming, besides a possibility of introducing sources of error, particularly when automated systems of activation analysis are required. These errors are frequently due to the different reaction rates in sample and standard caused by heterogeneous irradiation of such large volume due to flux gradient and neutron self-shielding. On the other hand, the relative method under Cd-filter has further disadvantages related to the Cd-filter itself. It causes difficulties in reactor operation, depression in neutron flux gradient and a considerable amount of the Cd^{115} isotope activity. To eliminate such difficulties a direct (absolute) method was considered (32), which is based on the irradiation of standards prepared from known weights of the elements to be determined by reactior neutron flux and the measurement of induced gamma-activities. The principle of this method involves the use of the well known equation

$$A = \frac{\sigma \theta \phi W N (1 - e^{-\lambda t}) e^{-\lambda t}}{M}$$

where

A = The disintegration rate of a radioisotope formed by neutron activation
σ = Activation cross-section
θ = Natural isotopic abundance of the target nuclide
ϕ = Reactor neutron flux
W = Weight of the target element to be determined
N = Avogadro's number
λ = Decay Constant of the radioisotope formed
M = Atomic weight of the target element
T = Irradiation time
T = Decay time

The results obtained using this equation suffer from accuracy compared to those obtained with the relative method due to the uncertainty which arises from using the thermal cross-section σ instead of effective cross-section σ_e, which is related to both thermal and epithermal components of the irradiated reactor neutron flux. Therefore a single comparator method based on the irradiation and counting a

known weight of an element used as a neutron flux monitor to avoid the influence of the variation of experimental parameters has been discussed (2). This method is often applied in activation analysis, when many elements were determined simultaneously or when samples and standards could not be irradiated together (1). A similar method (3) is applied using elements present in known quantities in the matrix itself as internal standard. None of this work was critically evaluated. However, the important advantages that could be gained by the use of a single comparator method for routine determination of many elements have encouraged Girardi et al. (11) to study the accuracy, precision and limits of applicability of this method for reactor neutron activation. In this evaluation all the treatment of the activity measurements was limited to the preliminary evaluation of a constant K, calculated from all nuclear constants involved in activation and in measuring the photopeak counting rates. The accuracy of the results depends on the accuracy of the determination of the quantities appearing in this study and the constancy of the K values with time, which mainly depend on the irradiation position, since a change of irradiation position leads to a change of the thermal to epithermal (Φ_{th}/Φ_{ep}) neutron flux ratio. Therefore, K values have to be corrected accordingly. De Corte et al. (12) have suggested a correction for K values without measuring the Cd-ratio, from the specific activities induced from two or more isotopes with well known resonance integrals (I_o) and thermal cross-section (σ_o) values. The discrepancy for all the above mentioned approaches in handling the single comparator method lyes in using as a reference standard an element with relatively high I_o value which leads to a remarkable change in sensitivity for any change in the irradiation position without considering the Westcott (19,20) correction.

Therefore the coupling of the epithermal neutron activation analysis with the monostandard method for elements with relatively high I_o values and using the monostandard of the same category (Co or Au) could overcome the difficulties mentioned above. In this way not only the difficulty due to changing irradiation position is eliminated but also the number of determinable elements is increased. At the same time, the sensitivity and accuracy are improved for many trace elements and the use of big cadmium capsules avoided. Many authors (33-45) have used this method in determining especially the trace elements in geological and biological materials. The irradiation of such materials with a whole reactor spectrum of neutrons produces a large number of gamma-activities of some radionuclides which interfere the γ-activity measurement of trace elements and increase their limit of detection and determination, while the activation with epithermal neutrons helps in reducing the unfavourable effect of the mentioned interfering activities without any chemical processing.

The monostandard epithermal neutron activation analysis is based on a suppression of the activity of nuclides having low I_o/σ_o values, namely nuclides following the 1/V law in the epithermal neutron energy region, in favour of nuclides having high I_o/σ_o values when thermal neutron are excluded. Most of the nuclides producing macroactivities in biological as well as geological materials in neutron activation are Na^{23}, K^{41}, P^{32}, Ca^{46} and Fe^{58}. On the other hand, many trace elements have nuclides with high resonance integrals. This fact offers more feasible determination of such trace elements especially when using Ge(Li) γ-spectrometry. Theoretical aspects of the approach and its application to the analysis of 17 trace elements beside K and Na in 17 different Egyptian granite rock samples are outlined.

2. Theoretical

The reaction rate per atom measured with reactor neutrons is affected by two components of neutron flux. A thermalized flux with a Maxwellian flux distribution characterized by its neutron temperature, T, shows a maximum for a velocity V_o = 2200 m/sec, corresponding to a kinetic energy E = KT, where K is Boltzmann's constant plus an epithermal or resonance flux whose energy distribution is assumed to be proportional to 1/V, particularly in a water-moderated reactor in the absence of epithermal absorption effects, extending from a lower limit, E_L to the fission energies. $E_L = \mu KT$, with μ = 5 (19) for D_2O reactor and 3 for a graphite reactor, where E_L = 0.17 eV (46). The thermal neutron spectrum does not show a perfect Maxwellian distribution due to the strong absorption of lower energy neutrons, and the lack of thermal equilibrium in the reactor medium due to capture and leakage. This component may be eliminated using a Cd-filter, since it has a very high absorption cross-section for thermal neutrons and allows the passage of neutrons above a certain energy E_c, which is dependent on shape and thickness of the Cd-filter. E_c = 0.55 eV for a small cylindrical Cd-cover with 1 mm thickness. From this introduction it is clear that for whole reactor neutrons contributing to a given nuclear reaction, the reaction rate per atom, induced from an isotope with a thermal cross-section for 2200 m/sec neutrons σ_o, and epithermal cross-section or so-called resonance integral I_o is given by

$$R = \Phi_{th}\,\sigma_{th} + \Phi_{ep}\,I_o \qquad (1)$$

where

Φ_{th} = thermal neutron flux

Φ_{ep} = epithermal flux per unit ln E

$\tilde{\sigma}_{th}$ = cross-section for subcadmium neutrons, ($\tilde{\sigma}_{th} = g\,\sigma_o$)

According to Westcott (19) the reaction rate per atom is given by

$$R = \Phi_o \hat{\tilde{\sigma}}(T) = nV_o \tilde{\sigma}_o \left[g(T) + r\sqrt{T/T_o}\ S_o \right] \qquad (2)$$

where

$\Phi_o = nV_o$ - neutron flux defined as the total neutron density times the 2200 m/sec velocity

$\hat{\tilde{\sigma}}(T)$ = effective cross-section

g(T) = parameter which represents the departure of the cross-section from the 1/V law in the thermal region (g(T) = 1 if nuclide obeys the 1/V law in this energy region) and which can be calculated from the expression (47)

$$g(T) = (1/\tilde{\sigma}_o V_o) \int_o^\infty \left[(4/\sqrt{\pi})\ (V^3/V_T^3)\ e^{(-V^2/V_T^2)} \right] \tilde{\sigma}_{(v)}\ dv \qquad (3)$$

or

$$g(T) = \frac{2}{\sqrt{\pi}\sqrt{E_o}\ \tilde{\sigma}_o} \int_o^\infty \sqrt{E}\ \tilde{\sigma}_{(E)}\ \sqrt{E/E_T}\ e^{(-E/E_T)}\ dE/E_T \qquad (4)$$

where

$E_T = E_o\ T/T_o$, E_o = 0.0253 eV and T_o = 293.6 °K.

The g(T)-functions for about 50 non 1/V reactions have been calculated in the temperature range from 0 to 2000 °K in the literature (48). $r\sqrt{T/T_o}$ is the epithermal index which refers to the epithermal flux. It is zero for a pure thermal flux and can be determined from the measurement of the Cd-ration (C_R) of a monitor nuclide

$$r\sqrt{T/T_o} = g(T)/\left[(C_R - 1)\ S_o + 4\ C_R \sqrt{E_o/\pi E_c} \right] \qquad (5)$$

where

S_o - parameter which represents the ratio of the resonance integral and thermal cross-section, such that

$$S_o = \frac{2}{\sqrt{\pi}\,\tilde{\sigma}_o} \int_{\mu KT}^{\infty} \left[\tilde{\sigma}(E) - g(T)\,\tilde{\sigma}_o \sqrt{E_o/E} \right] dE/E = (2/\sqrt{\pi})\,(I'_o/\tilde{\sigma}_o) \qquad (6)$$

The epicadmium resonance integral (I'_o) can be determined by measuring the Cd-ratio of the nuclide of interest at the irradiation position, where the epithermal index ($r\sqrt{T/T_o}$) is already known.

$$(2/\sqrt{\pi})\,(I'_o/\tilde{\sigma}_o) = \left[1/(C_R - 1)\right] (g(T)/r\sqrt{T/T_o} - 4\,g(T)\,C_R \sqrt{E_o/\pi E_c}) \qquad (7)$$

The epithermal index can be determined either with Eq. (5) or as mentioned in Part I of this report, it is preferable from the irradiation without Cd-cover of two different monitor nuclides, one sensitive to thermal activation and the other sensitive to epithermal activation; by the relation

$$r\sqrt{T/T_o} = (g_1(T)\,\tilde{\sigma}_{o1} - g_2(T)\,\tilde{\sigma}_{o2}\,R) \,/\, (S_{o2}\,\tilde{\sigma}_{o2}\,R - S_{o1}\,\tilde{\sigma}_{o1}) \qquad (8)$$

where

$R = \hat{\tilde{\sigma}}_1 / \hat{\tilde{\sigma}}_2$

which may easily be determined by the activity ratio of monitor 1 and monitor 2.

Actually the two neutron components of the whole reactor (thermal and epithermal) neutron flux overlap each other at a neutron energy of 0.5 eV, so that a more precise value of the resonance integral (I'_o) is defined either by relation (9) or relation (10) as follows (4,5):

$$I'_{o1} = \int_{\mu KT}^{\infty} (\tilde{\sigma}(E) - g\,\tilde{\sigma}_o \sqrt{E_o/E})\, dE/E \qquad (9)$$

or

$$I'_{o2} = \int_{\mu KT}^{EC} (\tilde{\sigma}(E) - g\,\tilde{\sigma}_o \sqrt{E_o/E})\, dE/E + \int_{Ec}^{\infty} (\tilde{\sigma}(E) - g\,\tilde{\sigma}_o \sqrt{E_o/E})\, dE/E$$

$$= \Delta I'_o + I'_o \qquad (10)$$

where I'_o is the epicadmium resonance integral excluding the 1/V part, and $\Delta I'_o$ is the part shielded by a Cd-filter excluding the corresponding 1/V part. The difference between I'_{o1} and I'_{o2} is significant only if there are resonances at energies near E_c, which is rare case.

The approximate resonance integral I_o, which includes the 1/V tail, is of more practical importance in epicadmium activation. I_o is given by

$$I_o = \int_{E_c}^{E_{max}} \sigma(E)\, dE/E \qquad (11)$$

From this equation the dependence of I_o on the Cd-filter used, as well as on the maximum neutron energy can be noticed. Since in this case only those neutrons which are not absorbed by Cd take part in the activation process. For irradiation under Cd-filter, the thermal component disappears and the reaction rate R in Eq. (1) takes the form (49)

$$R = \phi_{ep} I_o = \phi_{ep} (I'_o + 2\, g\, \sigma_o \sqrt{E_o/E}) \qquad (12)$$

Since E_o = 0.0253 eV so that for E_c = 0.55 eV the reaction rate is given by

$$R = \phi_{ep} (I'_o + 0.43\, \sigma_{th}) \qquad (13)$$

The Cd-ratio C_R is

$$C_R = \frac{\phi_{th}\, \sigma_{th} + \phi_{ep}\, I_o}{\phi_{ep}\, I_o} \qquad (14)$$

And according to Kim et al. (50) σ_{th} can be written as

$$\sigma_{th} \approx g\, \sigma_o + \frac{\phi_{ep}}{\phi_{th}} \int_{\mu KT}^{E_c} \sigma(E)\, \frac{dE}{E} \qquad (15)$$

$$= g\, \sigma_o + \frac{\phi_{ep}}{\phi_{th}} (I'_o - I_o) \qquad (16)$$

Eq. (16) may be written as

$$g\, \sigma_o = \sigma_{th} - \frac{\phi_{ep}}{\phi_{th}} (I'_o - I_o) \qquad (17)$$

Since the difference between σ_{th} and $g\, \sigma_o$ is small for a 1/V absorber, an approximate value can be used for the determination of σ_o for the 1/V absorber according to the following relation

$$\tilde{\sigma}_o \approx \int_{\mu KT}^{E_c} \tilde{\sigma}(E)\, dE/E \qquad (18)$$

An accurate value for $\tilde{\sigma}_o$ can be determined using Eq. (17) if the value $(I'_o - I_o)$ is known. For the condition of KT = 0.025 eV, E_c = 0.45 eV, and Φ_{ep}/Φ_{th} = 1/13, Halperin et al. (22) gave $I'_o - I_o = 0.4\ \tilde{\sigma}_o$ when E_c = 0.4 eV, whereas Macklin et al. (51) report 0.44 $\tilde{\sigma}_o$ with a cadmium filter of 0.5 mm as a better value. Therefore, the correction for the reaction rate due to the portion of 1/E spectrum between the lower limit of 1/E distribution E_L = 5 KT (μ = 5), and the effective cadmium cut-off E_c is calculated according to the following Equation (50):

$$\tilde{\sigma}_o = \tilde{\sigma}_{th} / (g + 0.45\, \Phi_{ep}/\Phi_{th}) \qquad (19)$$

The cadmium cut-off is thus used here to divide the thermal and epithermal reaction rate. Hence, $\tilde{\sigma}_{th}$ in Eq. (15) can be directly determined by irradiating the element in question without and with a Cd-filter, using the relation

$$R_{(total)} - R_{(epi)} = R_{(th)} = \Phi_{th}\, \tilde{\sigma}_{th} \qquad (20)$$

For the final calculation of the true thermal cross section, $\tilde{\sigma}_o$, using Eq. (19), the g value can be taken from literature (48), and Φ_{ep}/Φ_{th} is determined by measuring the Cd-ratio C_R of an appropriate monitor whose $\tilde{\sigma}_{th}$ and I_o are well known, using Eq. (14). The ratio, Φ_{ep}/Φ_{th} cannot be determined exactly, if the value of $\tilde{\sigma}_{th}$ is not known. In this case, the true thermal cross-section may be used and the flux is then given by (50) :

$$\Phi_{ep}/\Phi_{th} = g\, \tilde{\sigma}_o / (C_R - 1)\, (I_o - 0.45\, \tilde{\sigma}_o) \qquad (21)$$

This equation can be applied to a monitor such as Co or Au using the true thermal cross-section and the resonance integral above the epicadmium cut-off.

For an epithermal (epicadmium) neutron flux Φ_{ep} contributing to a given nuclear reaction, the photopeak counting rate A, induced from an isotope with a resonance integral I_o is given by

$$A = \Phi_{ep}\, I_o\, m\, \alpha \qquad (22)$$

where

m = weight of the element

α = NfbESD/M

N = Avogadro's number

f = fractional abundance of the isotope

b = absolute branching ratio of the measured γ-line

E = efficiency of the detector for that line

M = atomic weight of the element

S = $1-e^{-\lambda t_1}$ saturation factor

D = $e^{-\lambda t_2}$ decay factor

t_1 = irradiaton time

t_2 = decay time

λ = decay constant

If a 1/V monostandard with well known I_o value e.g. Co or Au is used the amount m of any of the unknown elements present in the irradiated sample can then be calculated from

$$m = \frac{I_o^* \cdot m^* \alpha^* A}{I_o \alpha A^*} = \left(\frac{I_o^* m^* \alpha^*}{A^*}\right) \frac{A}{I_o \alpha} = K \left(\frac{A}{I_o \alpha}\right) \qquad (23)$$

where (*) refers to the standard. If I_o for an element is not known with accuracy, it can be determined from Eq. (23) directly by simultaneously irradiating known amounts of that element and the standard under a Cd-filter similar to that subsequently used for analysis.

3. Experimental

Preliminary investigation for 17 different granite rock samples from Egypt has been performed using X-ray fluoresence to obtain a semiquantitative form on sample composition. For epithermal NAA, samples of about 150 mg were wrapped in 30 mm x 30 mm sheets of pure aluminium foil and packed in a 1 mm thick cadmium can with dimensions 20 mm internal diameter, by 40 mm internal height which allows for the 17 samples and the monostandard (Au) to be irradiated together. For epicadmium ratio and flux index ($r\sqrt{T/T_o}$) determination, Au-foils have been irradiated with and without Cd-filter. Irradiations were carried out for 1 hour in the Triga-II reactor of the Institute of Nuclear Medicine, DKFZ at Heidelberg

with a steady state power of 250 KW. After irradiation the samples and standard were allowed to cool for 2 days to permit the decay of undesirable short-lived isotopes.

The gamma-ray spectra of the cooled samples and standard (with and without Cd-filter) were measured for 50 min using a Ge(Li) spectrometer already described in Part I of this report. All the spectra measured were recorded on disk and processed on the PDP-11/34 computer connected to the measuring system. Subsequently the processed data are printed out and the spectra are plotted using Hewlett Packard printer and X-Y recorder.

The energy as well as the efficiency calibration of the detector have been determined experimentally using a number of radionuclides emit gamma-rays covering the whole energy range included in the present study. The efficiency values for each gamma-ray energy in the range up to 2000 keV as well as efficiency curves for 10 cm and 40 cm sample-to-detector geometries are given in Part I.

The energy calibration is based on the following simple relation

$$\text{channel number} = C_1 + C_2 \cdot E$$

where E is the energy in keV, C_1 and C_2 are the two calibration parameters.

To obtain an initial estimate of these calibration parameters, one measures the channel number at the peak maximum of two intense γ-ray lines, one in the low energy part (279 keV of Hg^{203}) and one in the high energy part of the spectrum (1332 keV of Co^{60}). The calibration parameters are then calculated as:

$$C_1 = \frac{CH_1 \cdot E_2 - CH_2 \cdot E_1}{E_2 - E_1}$$

$$C_2 = \frac{CH_2 - CH_1}{E_2 - E_1}$$

where CH_1 and CH_2 are the channel numbers of the peak maximum of the peaks with energy E_1 and E_2, respectively.

For efficiency calibration (at 10 cm geometry where all the measurements were carried out) the following formulas are used:

For energies lower than 279 keV:

$$\log (Eff) = -5.9843 + 22.0357 \times \log (E) - 3.2464 \times \log (E)^2 + 0.1345 \times \log (E)^3$$

while higher than the cross-over energy 279 keV:

$$\log (Eff) = 1.2444 - 1.4526 \times \log (E) + 0.0352 \times \log (E)^2$$

The conditions under which the irradiation were carried out are estimated using Eqs. (1), (5), (6) and (14) with the following flux values:

$$\phi_t = 1.03 \times 10^{13} \text{ n/cm}^2 \cdot \text{sec}$$
$$\phi_{ep} = 1.95 \times 10^{11} \text{ n/cm}^2 \cdot \text{sec}$$
$$\phi_{th} = 1.01 \times 10^{13} \text{ n/cm}^2 \cdot \text{sec}$$

flux index r $T/T_o = 0.016$, $S_o = 17.4$ and the constant K for the monostandard (Au) appears in Eq. (23) and is equal to 5.13×10^{-12} for the present irradiation conditions.

4. Results and discussion

The X-ray spectra for six samples selected from the 17 granite rock samples are depicted in figures 7 through 12. Such semiquantitative analysis gave an idea about the elements present in those rock samples, such as Y, Sr, Rb, Ti, Zr, As, Fe, Cu, Zn, Mn, K, Ga, and Ca. Many of these elements are trace elements with relatively high I_o values which have favourable epithermal activation properties. Therefore irradiation of the granite samples were carried out under a cadmium filter using gold which is of the same category as monostandard, while I_o values are used as the effective cross-sections. Co as a 1/V absorber could be a convenient standard, but in order to obtain a large epithermal effect in a short irradiation (1 hour), Au is preferable. Figs. 13-15 show the gamma-spectra of three typical granite samples measured at different decay times. These gamma-spectra demonstrated the advantages of epithermal neutron activation for many trace elements such as As, Au, Ag, Ga, Eu, Sm, SN, Hf and W as one way to decrease the interfering activities. Also a number of elements with $\sigma_o > I_o$ such as Na, K and Zr were found to be sensitive enough to be detectable by epithermal activation.

For calculations using Eq. (23) to determine the concentration of the elements present in the irradiated samples, I_o values were taken from the literature (23, 47). Results of determining 18 trace elements beside Na and K for the 17 granite rock samples are given in Tables (4) and (5). The statistical error in each of these values does not exceed 10 %. All calculations presented here based on utilising the net γ-peak area of the concerned isotope given by the PDP-11 computer of the measuring system. For further processing a small 11C Hewlett-Packard calculator has been used. The program used by the PDP-11 computer to analyse the measuring data is a FORTRAN program developed by CANBERRA company for the analysis of gamma-spectra, by iterative non-linear least-squares fitting of highly complex γ-ray spectra as obtained with the Ge(Li) detector. The program provides net peak intensities corrected for background and peak overlap of the different elements analysed. For routine work, epithermal neutron activation analysis (ENAA) cannot compete with conventional reactor neutron activation analysis (RNAA) because of the special sample handling requirements (Cd-cover for each sample and Cd-ratio monitor) and the fact that certain elements (Sc, Co, Nd, Sm, Eu, Lu, Cr, LA, Fe, Ce) are still better to be determined by RNAA method. However, the epithermal technique overcomes the RNAA technique by greatly improving the sensitivity and accuracy with which some elements can be determined particularly (Zn, Rb, Gd, Ba, Tb, Tm, Yb, Sb, Cs, Hf, Ta, Th). Moreover, the ENAA method provides data for some elements (U, Sr, Mo, Ni) which are difficult to determine by the RNAA method.

5. Conclusions

Among all the determined elements, uranium and thorium are of especial interest for the purpose of analysing the rock samples. The advantages of their analysis by ENAA compared with RNAA are due to their high I_o/σ_o ratios (> 100 for U and > 10 for Th). Thorium is determined by measuring the 312 keV γ-line of Pa^{233} which is the β-decay of the reaction Th^{232} (n, γ) Th^{233} with resonance cross-section (I_o) value 85 barn. In case of U, its analysis was through the 277.6 keV γ-peak of Np^{239} which is the β-decay of the reaction U^{238} (n,γ) U^{239} with effective value of I_o, 400 barn (49).

The analysed data given in Tables (4) and (5) show that U is present in nearly all the granite rock samples of group 2, and its concentration ranging from 7-13 ppm while in group 1 it is present only in 5 rock samples with different concentrations

from 7-17 ppm, while Th is present only in one rock sample from group 1 with concentration 18 ppm and in 4 samples of group 2 with concentrations ranging from 7-63 ppm. In general all the granite rock samples analysed in this work show similarity in their elemental composition with different concentrations. However, the treatment of the data concerning the distribution of the elements in these rock samples and their geology will be discussed in more detail in a future publication.

So the method of monostandard epithermal neutron activation analysis proved its applicability and sensitivity for the analysis of trace elements bearing samples and could certainly be valuable for the nondestructive analysis of precious and archaeological materials.

III. Prompt Gamma-Ray Neutron Activation Analysis (PGNAA) Facility Testing by Sm, Gd and Mn Determination in Rock Samples

1. Introduction

Despite the strengths of RNAA in the analysis of complex samples further samples have restrictions that make it impossible to insert them into reactors e.g. they might decompose or explode, their size is physically too large, or the heating, radiation damage, and residual activity are undesirable. To overcome these problems many authors (52-62) have investigated the use of prompt gamma-ray neutron activation analysis (PGNAA) technique. In this technique one measures γ-rays emitted while the sample is being irradiated with neutrons.

In PGNAA, when a sample is irradiated with slow neutrons the (n, γ) reaction is generally the most favourable nuclear reaction which can occur. Following neutron capture, the resultant compound nucleus is left in an excited state with energy essentially equal to the neutron binding energy of the compound nucleus (in general, 5-11 MeV). Decay occurs promptly within about 10^{-14} sec from the excited state to the ground state, normally through several intermediate states, by the emission of several γ-rays. In general, neutron capture gamma-ray spectra are complex, consisting of both high and low energy gamma-radiations. Thus, nearly every neutron capture yields γ-rays that are potentially usable for analysis for the capturing element. But the radioactive nuclides formed by neutron capture are not necessarily the same used by RNAA, in such a way that the product nuclei may be stable, have very short or long half-life or emit no intense γ-radiation. For example, Cd has an enormous neutron capture cross-section for the reaction Cd^{113} (n, γ) Cd^{114}, where the product nuclide (Cd^{114}) is stable and is of no use in RNAA while in PGNAA prompt γ-rays from neutron capture by Cd^{113} can possibly be measured. Other elements, such as (S and P) after neutron irradiation are pure beta-emitters, can also be determined non-destructively by capture γ-ray analysis.

For irradiated nuclide the rate R for neutron capture -ray analysis is given by

$$R = N \cdot \phi \cdot \sigma \qquad (1)$$

This relation shows that capture γ-rays production is directly proportional to the total neutron capture cross-section (σ) of the sample. In a sample containing several elements, the quantity (σ/A) (63) for each element provides an indication of the relative sensitivities for measuring these elements using a neutron capture γ-ray technique. A more useful measure of the relative sensitivity is given (64,65) by combining the neutron absorption values, σ/A, with the number of gamma-rays I,

of a given energy produced per 100 neutrons captured, which indicate spectral response. Thus, a sensitivity factor S equal to

$$S = I\sigma/A \qquad (2)$$

is more closely indicating a relative number of γ-rays emitted for a given energy. The maximum values of ($I\sigma/A$) for the naturally occuring elements for the energy range from 0 to 1.5 MeV and form 3 to 10 MeV are presented in Tables 6 and 7 taken from earlier work by Henkelmann et al. (60).

These tables show that the low-energy values are higher for most elements while in the high energy range many of the rare earth elements have no significant peak with an intensity of more than 1 %. This indicates that a neutron capture γ -ray analysis technique is in principal a method for analysis of major conditions. This means, trace analyses (ppm) being possible only for a few specialized cases, where high neutron flux is used.

Although a reactor provides the most intensive neutron flux for such studies, it is still inconvenient to apply it for such routine work as industrial or in situ analysis. Therefore many authors (66-69) have pointed out the possibility of using isotopic neutron sources giving relatively high neutron yields. Among these the most widely isotopic neutron source used in the field of activation analysis is Cf-252 source, which is a spontaneous fission neutron emitter. Cf^{252} is currently manufactured by irradiating plutonium targets in a reactor. Starting with Pu^{239}, the production of Cf^{252} requires a series of 13 neutron captures. Cf^{252} has a half-life of 2.65 years and decays by alpha-particle emission or by spontaneous fission giving neutron flux of 2.34×10^{10} n/sec from one gram. The unmoderated neutron spectrum of Cf^{252} is roughly the same as that of U^{235} fission. Cf^{252} neutron source with strength of several milligrams might yield a usable thermal neutron flux of $\sim 10^8$ n/cm² · sec compared with a flux of 10^{13} n/cm² · sec available from the reactor. Therefore many laboratories (70-75) have constructed especial facilities for using Cf^{252} in exploring elemental analysis applying the neutron capture γ -ray method. At the Institute of Radiochemistry, KfK, a facility for applying the PGNAA technique has been designed and assembled recently using two Cf^{252}-sources of 27 and 15 µgm in a cubic container of paraffin and plexiglass moderators with volume of 1 m³. This facility has been used in estimating B, Cl and P contents in industrial and reference materials (76).

This work deals with testing the applicability and sensitivity of this facility using only one 27 μg Cf^{252} neutron source of strength 6 x 10^7 n/sec for quantitative analysis of rock samples (phosphate and monazite). These two samples have been chosen as extensive reactor neutron activation anlysis (RNAA) data are available from them and thus would form a suitable study for comparison. Though the analysis of these samples by the latter technique has shown the presence of more than 20 elements, only three of them (Sm, Gd and Mn) are amenable for comparison by PGNA method using Cf^{252} neutron source due to high cross-sections of Sm and Gd and high abundance of Mn in the samples. Fe in spite of its high content in the rock samples was excluded as a refence testing element because of its high background contribution from the surrounding materials of the set-up. The analysis by (PGNAA) facility in this work is concerned with two representative samples one each from the phosphate and monazite ores.

2. Experimental

The PGNAA facility installed at the laboratory has been used in the present study. Full detaiis of the system have been reported elsewhere (76). A 27-μg Cf^{252} neutron source (6 x 10^7 n/sec) was moderated and shielded with paraffin and plexiglass and used with a Ge(Li) detector in an internal target arrangement for capture-gamma-ray analyses. The detector was covered by a closed end jacket of Li^6-carbonate (with 95.58 atom % Li^6) of 1 cm thickness for protection against scattered neutrons. The neutron flux density at the target when the irradiated source at its nearest position from the target was estimated as 10^5 n/cm · sec. The prompt γ-rays emitted by the irradiated samples were measured using a Ge(Li) detector with a relative efficiency of 13.5 % and resolution of 1.95 keV FWHM at 1332 keV of Co^{60}. The detected signals from the detector were passed after suitable amplification to 4096 multichannel analyzer which is connected to plotter and printer for data analyses.

The energy calibration of the detector for low energy range up to 2000 keV was established using the gamma-lines of standard sources Cs^{137} (662 keV), Co^{60} (1173 and 1332 keV) and the three energy peaks of hydrogen from the measured background spectrum. These peaks are the full energy line 2223.1 keV, the single escape line 1712.1 keV and the double escape line 1201.1 keV arising from the pair production process of the full energy gamma-line of hydrogen with the Ge(Li) detector. The calibration fitting was done by the computer and the accuracy was 0.2 keV.

For calibration purposes, liquid standard samples at different concentrations ranging from 100 µg/l to 500 µg/l in case of Sm and Gd, while for Mn from 1000 µg/l to 5000 µg/l were used. The standard solutions were irradiated and counted for 100 min each. The spectra were printed out and the net photopeak areas were determined by the computer.

About 20 g of monazite and 12 g of phosphate samples were packed into precleaned 50 ml polyethylene bottles. Each sample was then irradiated in the PGNAA set-up for approximately 17 hours, where the measured gamma-rays were printed out and analyzed graphically. The background for each sample was measured for the same period.

3. Results

An overall sketch of the PGNAA facility used in this study is depicted in Fig. (16) showing the relative positions of the Ge(Li) detector, shield, two Cf^{252} neutron sources and the sample. The two Cf^{252} sources shown in the figure have been replaced by one source of strength $\sim 6 \times 10^7$ n/sec for performing this investigation. The prompt gamma-ray photopeaks of 334 and 439 keV for Sm, 247 and 1185 keV for Gd and 847 and 1810 keV for Mn are chosen to perform these investigations due to their high sensitivity as given by Table (8), and earlier studies (77-79) were proven to be the best. In case of Sm and Mn both photopeak areas were combined while for Gd only the 1185 keV peak was used due to the relatively high background contribution for the 247 keV line. The background was estimated by constructing a base line for each photopeak taken independently from the background measurement of a reference sample. The net peak area values of the gamma-ray lines for elements Sm, Gd and Mn have been plotted against the concentration percentage values as shown in Figs. (17), (18) and (19), respectively. These calibration curves are necessary for the determination of the existing concentration values of these elements in the monazite and phosphate ore samples which were irradiated and measured under the same conditions. The prompt gamma-ray spectra for thermal neutron capture in monazite and phosphate ore samples are shown in Figs. (20) and (21), respectively. The data analysis from these two spectra represents the percentage values of elements Sm, Gd and Mn in µg/gm (ppm) in the ore samples determined by the PGNAA facility. The tabulated results for these analyses and those obtained by the RNAA method for comparison are presented in Table (9).

4. Discussion

For analytical purpose using neutron capture gamma-ray method, two basic configurations are possible concerning the analysed sample and neutron source position. In the first case, the sample is brought near the source and the detector is kept some distance away for shielding purposes is known by "internal geometry" (80). This configuration results more gamma-intensity from the sample but with a loss in solid angle subtended by the detector. In the second configuration, the sample is placed some distance away from the source while the detector is carefully shielded and close to the sample. In this case, the sample emits few numbers of gamma-rays but more flexibility in detector arrangement. The latter method (external geometry) (81) allows better shielding for the detector at right angles out of the neutron beam for reducing both the gamma-background and the neutron effects on the detector. Therefore, the external geometry has been preferred for analytical studies especially with a high-yield research reactor. But in case of using Cf^{252} source the situation is different since Cf^{252} offers a convenient point source of neutrons for laboratory capture-gamma-ray experiments as well as for field analyses. However, the neutron yield of a small Cf^{252} source (few µgs) usually used in such studies is not large enough to collimate the emitted neutrons from the source as is the case in using the reactor. Therefore, to increase the number of captures from a point Cf^{252} source it is necessary to use the internal geometry configuration. The design and construction of the PGNAA facility used in this work was based on this geometry as shown in Fig. (16). However, the shielding was designed to verify enough personal protection, reducing gamma-emissions from surrounding structural materials and minimizing neutron damage to Ge(Li) detector.

The experimental data obtained by this set-up are tabulated in Table (9). The table shows a difference between the measured concentration values of Sm, Gd and Mn in the rock samples and those obtained by RNAA method with about 25 %. This deviation should be mainly due to the relatively low signal-to-background ratio ($\sim$ 0.1) found for the gamma-peaks of concerned elements by using our set-up. Also the concentration level of Sm in its phosphate sample was difficult to be evaluated with a reasonable accuracy, therefore its value was excluded. The prompt gamma-ray spectra of the rock samples show the absence of the low energy gamma-line (247 keV) of Gd, Fig. (20) as well as the 334 keV and 439 keV gamma-lines of Sm in Fig. (21) in spite of the high detection efficiency and high sensitivity of these gamma-lines. These discrepancies in the measured data obtained are mainly due to

i) the small Cf^{252} neutron source ($\sim$6 x 10^7 n/sec) used giving small intensity peaks,

ii) the high contribution of Compton tail background producing minimum signal-to-background ratio as shown in Figs (20) and (21).

Since the source of background and its contribution varies for different energy regions the detector shielding and the construction materials used in the present set-up may have different effects for each analyzed element. The different contributions of background sources are discussed in detail by Vartsky et al. (83). We can summarize the contribution of each background source to the total background as applicable to our present set-up as follows:

1. Natural background
2. Source and facility induced background
3. Background due to scattering
   a) Cf^{252} source gamma-rays scattered by the target
   b) neutron scattered by the target
   c) contribution from neutron capture hydrogen gamma-rays produced by the moderating materials and their Compton scattering in the detector for full, double and single escape peaks 2223.1, 1712.1 and 1201.1 keV, respectively of H.

5. Conclusions

It is clear from the discussion that the constructed shielding of the PGNAA facility has succeeded to a large extent in reducing the background contribution from the facility and surround materials to a minimum while the interferences from scattering as mentioned under 3. still constitute the largest fraction of the contributed background.

Since most of the interference from this phenomena occurs in the low energy region below 2223.1 keV of the full hydrogen peak due to its Compton scattering in the Ge(Li) detector as well as the neutron capture in the detector in spite of its shielding with Li^6 jacket. Since Li^6 eliminates the thermal neutrons to the lowest level, still the fast neutrons are unaffected by the Li^6 shield and can penetrate the detector where they are captured after slowing down in it giving the reaction $Ge^{75}(n, \gamma)$ Ge^{74}. The energy levels of the product isotope resulting from this reaction have been investigated by Weitkamp et al. (84).

These background contributions can be reduced to a major extent by the following steps:

a) introducing about a 2.5 cm thick polyethylene layer before the Li^6-shield to slow down any stray fast neutrons which can hit the detector

b) setting-up between the neutron source and the target a conical collimator (83) made from polyethylene with thickness about 10 cm, containing a 1 cm thick lead sheet to obtain the optimal thermal neutron flux with low level of Cf^{252} gamma-rays.

While the intensity of the prompt gamma-ray peaks of the investigated elements measured by the PGNAA facility can be increased by using larger Cf^{252} source with neutron flux of the order to 10^8 n/sec and the detected solid-angle was enlarged by reducing the detector-target-distance.

Finally, it can be concluded that this facility is a valuable tool in the analysis of rock samples and further work is necessary to incorporate the suggestions reported in this work which should be of considerable value for more accurate analysis.

Acknowledgement

One of the authors (R. Zaghloul) is grateful to those members of the radioanalytical group, IRCH, who helped and supported him during this course of work. Many thanks to the authorities of the International Büro at KfA Jülich for financing the guest scientist period from June 2 to December 15, 1985. The sabbatical leave granted by the Egyptian Atomic Energy Authority is much appreciated. The same author is extremely thankful to Dr. J.I. Kim from the Institute of Radiochemistry, TU München, Garching, for his aids during performing the data analysis at the Center using his computer program of monostandard technique.

The authors thank Mr. J. Reinhardt for his help in preparing the X-ray analysis. They would furthermore like to thank the group of Triga II reactor at the Institute of Nuclear Medicine, KDFZ - Heidelberg, for arranging the irradiations.

References

1. F. Adams, J. Hoste, A. Speecke, Talanta, 10 (1963) 1243
2. R. Fukai, W.W. Meinke, Nature, 184 (1959) 815
3. D. Monnier, W. Haerdi, J. Vogel, Helv. Chim. Acta, 44 (1961) 897
4. J.I. Kim, H.J. Born, J. Radioanal. Chem. 13 (1973) 427
5. A. Alian, H.J. Born, J.I. Kim, J. Radioanal. Chem. 15 (1973) 535
6. D.L. Massart, J. Hoste, Anal. Chim. Acta, 42 (1968) 21
7. R.V. Linden, F. De Corte, J. Hoste, J. Radioanal. Chem. 20 (1974) 729
8. P. Lievens, R. Cornelis, J. Hoste, Anal. Chim. Acta, 80 (1975) 97
9. N. Tamura, Radiochem. Radioanal. Letters, 18 (1974) 135
10. F. De Corte, A. Speecke, J. Hoste, J. Radioanal. Chem. 9 (1971) 9
11. F. Girardi, G. Guzzi, J. Pauly, Anal. Chem. 37 (1965) 1085
12. F. De Corte, A. Speecke, J. Hoste, J. Radioanal. Chem. 3 (1969) 205
13. N.A. Dubinskaya, L.L. Pelekis, J. Radioanal. Chem. 9 (1971) 61
14. A. Simonits, F. De Corte, J. Hoste, J. Radioanal. Chem. 24 (1975) 31; 31 (1976) 467
15. R. Van der Linden, F. De Corte, J. Hoste, J. Radioanal. Chem. 13 (1973) 169
16. D.M. Linekin, J. Appl. Radiation Isotopes, 24 (1973) 343
17. M. Heurtebise, F. Montolay, J.A. Lubkowitz, Anal. Chem. 45 (1973) 47
18. R. Zaghloul, J. Radioanal. Nucl. Chem. (to be published)
19. C.H. Westcott, W.H. Walker, T.K. Alexander, 2nd Intern. Conf. Peaceful Uses of Atomic Energy, Geneva, 16 (1958) 70
20. C.H. Westcott, AECL-1101, 1960
21. H.D. Lemmel and C.H. Westcott, J. Nucl. Energy, 21 (1967) 417
22. J. Halperin, R.W. Stoughton, 2nd Intern. Conf. Peaceful Uses of Atomic Energy, Geneva, 16 (1958) 64
23. J.I. Kim, J. Radioanal. Chem. 63, No. 1 (1981) 121
24. E.M. Gryntakis, J.I. Kim, J. Radioanal. Chem. 29 (1976) 175; 42 (1978) 81
25. BNL-325, 3rd Ed. Vol. 1, 1973
26. E.M. Gryntakis, J.I. Kim, Radiochim. Acta, 22 (1975) 128
27. J.I. Kim, E.M. Gryntakis, H.J. Born, Radiochim. Acta, 22 (1975) 20
28. E.M. Gryntakis and J.I. Kim, J. Radioanal. Chem. 76, No. 2 (1983) 341
29. J.I. Kim and F. Adams, Radiochim. Acta 9 (1968) 61
30. E. Ricci, Anal. Chim. Acta, 79 (1975) 109
31. A. Travesi, J. Adrada and J. Talomares, Nuclear activation techniques in the life sciences, International Atomic Energy Agency, Vienna (1972) 89

32. F. Girardi, G. Guzzi, J. Pauly, Anal. Chem. 36 (1964) 1588
33. J. Kucera, Radiochem. Radioanal. Letters, 38, No. 4 (1979) 229
34. Z. Randa, Radiochem. Radioanal. Letters, 24, No. 3 (1976) 157
35. A. Alian, B. Sansoni, J. Radioanal. Chem. 59, No. 2 (1980) 511
36. H.G. Meyer, J. Radioanal. Chem. 7 (1971) 67
37. Z.B. Alfassi, J. Radioanal. Nucl. Chem. 90, No. 1 (1985) 151
38. P.A. Baedecker, J.J. Rowe, E. Steinnes, J. Radioanal. Chem. 40 (1977) 115
39. D.C. Borg, R.B. Segel, P. Kienle, L. Campbell, Intern. J. Appl. Radiat. Isotopes, 11 (1961) 10
40. M. Rakovic, Z. Prouza, Isotopenpraxis, 4 (1968) 11
41. D. Brune, P.O. Wester, Anal. Chim. Acta, 52 (1970) 372
42. N.V. Bagdavadze, L.M. Mosulishvili, J. Radioanal. Chem. 24 (1975) 65
43. B. Maziere, J. Gros, D. Comar, J. Radioanal. Chem. 24 (1975) 279
44. D. Brune, B. Bivered, Anal. Chim. Acta, 85 (1976) 411
45. A. Cesana, F. Rossitto, M. Terrani, J. Radioanal. Chem. 45 (1978) 199
46. D.J. Hughes, "Pile Neutron Research", Addison-Wesley (1953)
47. E.M. Gryntakis, J.I. Kim, J. Radioanal. Chem. 76, No. 2 (1983) 341
48. E.M. Gryntakis, J.I. Kim, Radiochim. Acta, 22 (1975) 128
49. A. Alian, B. Sansoni, J. Radioanal. Chem. 59 (1980) 511
50. J.I. Kim, F. Adams, Radiochim. Acta, 8 (1967) 165
51. R.C. MacKlin, H.S. Pomerance, Proc. Intern. Conf. on Peaceful Uses of Atomic Energy, Geneva, 5 (1956) 96
52. S.M. Lombard, T.L. Isenhour, P.H. Heintz, G.L. Woodruff, W.E. Wilson, Int. J. Radiat. Isot. 19 (1968) 15
53. E.S. Gladney, E.T. Jurney, D.B. Curtis, Anal. Chem. 48 (1976) 2139
54. S.M. Lombard, T.L. Isenhour, Anal. Chem. 40 (1968) 1990
55. E.T. Jurney, D.B. Curtis, E.S. Gladney, Anal. Chem. 49 (1977) 1741
56. M.P. Failey, D.L. Anderson, W.H. Zoller, G.E. Gordon, Anal. Chem. 51 (1979) 2209
57. D.L. Anderson, M.P. Failey, W.H. Zoller, W.B. Walters, G.E. Gordon, R.M. Lindstrom, J. Radioanal. Chem. 63 (1981) 97
58. E.S. Gladney, D.B. Curtis, E.T. Jurney, J. Radioanal. Chem. 96 (1978) 299
59. E.S. Gladney, D.B. Curtis, E.T. Jurney, Anal. Chim. Acta, 110 (1979) 339
60. R. Henkelmann, H.J. Born, J. Radioanal. Chem. 16 (1973) 473
61. R.C. Greenwood, Proc. 3rd Int. Symp. on Neutron Capture Gamma-Ray Spectroscopy and Related Topics, BNL, Upton, New York, Sept. 18-22 (1978)
62. H.K.L. Gupta, D.F. Boltz, Anal. Lett. 4 (1971) 161
63. R.C. Greenwood, J. H. Reed, IITRI-1193-53 (1965)
64. N.C. Rasmussen, Y. Hu Kai, T. Inouye, V.J. Orphan, AFCRL-69-0071 (1969)

65. D. Duffey, A. El-Kady, F.E. Senftle, Nucl. Instr. Methods, 80 (1970) 149
66. J. Wing, M.A. Wahlgren, Anal. Chem. 39 (1967) 85
67. M. Wahlgren, J. Wing, D.C. Stewart, Proc. Intern. Conf. Modern Trends in Activation Analysis, No. 80 (1968)
68. W.C. Reining, A.G. Evans, Proc. Intern. Conf. Modern Trends in Activation Analysis , No. 33 (1968)
69. Y. Kusaka, H. Tsuji, J. Radioanal. Chem. 5 (1970) 359
70. S. Uusitalo, E. Mäkinen, D.O. Riska, Proc. 4th (n, γ) Int. Symp. Grenoble, Sept. 7-11 (1981) 682
71. I.P. Matthews, N.M. Spyrou, Int. J. Appl. Radiat. Isot. 33 (1982) 61
72. C.G. Clayton, A.M. Hassan, M.R. Wormald, Int. J. Appl. Radiat. Isot. 34 (1983) 83
73. F.E. Senftle, R.J. Macy, J.L. Mikesell, Nucl. Instrum. Methods, 158 (1979) 293
74. A.B. Tanner, R.M. Moxham, F.E. Senftle, Nucl. Instrum. Methods, 100 (1972) 1
75. F.E. Senftle, D. Duffey, P.F. Wiggins, Nucl. Techn. 10 (1971) 204
76. A.M. Hassan, E. Gantner, E. Mainka, H. Ruf, U. Kuhnes, M. Mostafa, KfK-3387, July (1982)
77. S.M. Lombard, T.L. Isenhour, Anal. Chem. 40 (1968) 1990
78. S.M.Lombard, T.L. Isenhour, Anal. Chem. 41 (1969) 1113
79. E. Bieber, T.V. Egidy, O.W.B. Schult, Z. Physik, 170 (1962) 465
80. G.E. Thomas, D.E. Blatchinkey, L.M. Ballinger, Nucl. Instr. Methods, 56 (1967) 325
81. A.A. El-Kady, D. Duffey, Trans. Am. Nucl. Soc. 12 (1969) 42
82. J.P. Nichols, Nucl. Appl. 4 (1968) 382
83. D. Vartsky, K.J. Ellis, L. Wielopolski, S.H. Cohn, Nucl. Instr. Methods, 213 (1983) 437
84. C. Weitkamp, W. Michaelis, H. Schmidt, U. Fanger, Z. Physik, 192 (1966) 423

Table 1-a

Ge(Li) Detector Efficiency Values at Geometry 10 cm

E_γ, keV	Eff.	E_γ, keV	Eff.	E_γ, keV	Eff.
62.5	$2.8530\ E^{-3}$	531	1.5295	1099.3	7.4701
103.2	5.5467	559.1	1.4520	1115.4	7.3667
106.1	5.6350	563.9	1.4395	1120.5	7.3346
122	5.9123	572.9	1.4168	1121.4	7.3290
133	5.9360	602.7	1.3465	1173.2	7.0193
145.4	5.8440	604.6	1.3422	1188.9	6.9308
158.4	5.6500	609	1.3325	1221.5	6.7545
186.1	5.058	622	1.3047	1291.9	6.4044
189.9	4.9676	629.9	1.8835	1297.2	6.3796
208.4	4.0517	657.7	1.2341	1332.5	6.2195
238.6	3.0803	662	1.2261	1368.5	6.0649
277.6	3.001	685.7	1.1840	1460	5.7064
282.6	2.9340	743.4	1.0930	1524.7	5.4790
298	2.7740	766.4	1.0607	1596.2	5.2493
311.9	2.6445	795.8	1.0221		
320.1	2.5737	833.9	$9.7632\ E^{-4}$		
328.8	2.5025	835	9.7506		
344.3	2.3852	846.6	9.6200		
352.1	2.3300	879.3	9.2706		
388.3	2.1056	889.4	9.1680		
396	2.0634	908	8.9851		
411.8	1.9082	963	8.4866		
479.5	1.6961	966.2	8.4594		
487	1.6696	1001.1	8.1741		
496.3	1.6378	1077	7.6185		

Table 1-b

Ge(Li) Detector Efficiency Values at Geometry 40 cm

E_γ , keV	Eff.	E_γ , keV	Eff.	E_γ , keV	Eff.
62.5	2.7306 E^{-4}	531	1.54	1115.4	7.4689
103.2	4.9998	559.1	1.4654	1120.5	7.4358
106.1	5.0630	563.9	1.4532	1121.4	7.4300
122	5.2385	572.9	1.4309	1173.2	7.1100
133	5.2277	602.7	1.3617	1188.9	7.0185
145.4	5.1273	604.6	1.3575	1221.5	6.8370
158.4	4.9552	609	1.3480	1291.9	6.4727
186.1	4.4744	622	1.3204	1297.2	6.4470
189.9	4.4031	629.9	1.3043	1332.5	6.2805
208.4	4.0553	657.7	1.2504	1368.5	6.1195
238.6	3.5155	662	1.2425	1407.9	5.9527
277.6	2.9130	685.7	1.2005	1460	5.7457
282.6	2.8560	724.2	1.1382	1524.7	5.5081
298	2.7114	756.7	1.0905	1596.2	5.2678
311.9	2.5931	795.8	1.0381		
320.1	2.5280	833.9	9.9183 E^{-5}		
328.8	2.4625	835	9.9056		
344.3	2.3540	846.6	9.7731		
352.1	2 3030	879.3	9.4184		
388.3	2.0927	889.4	9.3141		
396	2.0529	908	9.1280		
411.8	1.9758	963	8.6191		
479.5	1.7026	966.2	8.5913		
482	1.6940	1077	7.7284		
496.3	1.6463	1099.3	7.5755		

Table 2

Physical Constants of the Elements Determined by the Monostandard Method

Element	Target nuclide	Natural abundance %	Product nuclide	Half-life	Thermal cross-section σ_0, barn	Resonance integral, I_0 barn	Main Gamma-rays energy, keV (absolute intensity)
As	As-75	100	As-76	26.4 h	4.3 ± 0.1	49.9 ± 4.4	559.1 (0.446), 657 (0.064)
Au	Au-197	100	Au-198	2.695 d	98.8 ± 0.3	1523 ± 7	411.8 (0.955)
Ce	Ce-140	88.48	Ce-141	32.5 d	0.57 ± 0.04	0.23 ± 0.02	145.4 (0.48)
Co	Co-59	100	Co-60	5.272 y	37.2 ± 0.2	58.26 ± 1.28	1173.2 (0.999), 1332.5 (0.999)
Cr	Cr-50	4.35	Cr-51	27.7 d	15.9 ± 0.2	1.44 ± 0.64	320.1 (0.202)
Cs	Cs-133	100	Cs-134	2.06 y	29.0 ± 1.5	410 ± 11	569.3 (0.154), 604.6 (0.976), 795.8 (0.854)
Eu	Eu-151	47.77	Eu-152	12.7 y	5935 ± 73	6442 ± 1549	344.3 (0.314), 778.9 (0.152)
Fe	Fe-58	0.31	Fe-59	45 d	1.15 ± 0.02	0.80 ± 0.10	1099.3 (0.565), 1291.9 (0.432)
Hf	Hf-180	35.22	Hf-181	42.5 d	12.6 ± 0.7	30.3 ± 2.4	133 (0.43), 482.0 (0.86)
K	K-41	6.70	K-42	12.36 h	1.46 ± 0.04	0.69 ± 0.04	1524.7 (0.18)
La	La-139	99.91	La-140	40.23 h	9.03 ± 0.33	10.15 ± 1.0	487.0 (0.430), 1596.2 (0.955)
Lu	Lu-176	2.60	Lu-177	6.7 d	2093 ± 50	500 ± 250	113.0 (0.066), 208.4 (0.011)
Na	Na-23	100	Na-24	15.03 h	0.530 ± 0.005	0.084 ± 0.0023	1368.5 (1.00)
Rb	Rb-85	72.17	Rb-86	18.7 d	0.46 ± 0.02	4.93 ± 0.61	1077 (0.088)
Sb	Sb-121	57.25	Sb-122	2.72 d	6.25 ± 0.2	197 ± 7	563.9 (0.66), 692.8 (0.063)
Sc	Sc-45	100	Sc-46	83.9 d	26.5 ± 1.0	0.60 ± 0.77	889.4 (1.00), 1120.5 (1.00)
Sm	Sm-152	26.63	Sm-153	46.8 h	206 ± 6	2902 ± 64	103.2 (0.28)

Table 2, continued

Element	Target nuclide	Natural abundance %	Product nuclide	Half-life	Thermal cross-section σ_o, barn	Resonance integral, I_o barn	Main Gamma-rays energy, keV (absolute intensity)
Sn	Sn-116	14.3	Sn-117	14 d	0.006 ± 0.002	0.49 ± 0.02	158.4 (0.65)
Ta	Ta-181	99.998	Ta-182	115.1 d	21.0 ± 0.7	717 ± 58	1188.9 (0.165), 1221.3 (0.274)
Tb	Tb-159	100	Tb-160	72.3 d	25.5 ± 1.1	434 ± 35	298 (0.274), 879.3 (0.30) 966.2 (0.255)
Th	Th-232	100	Pa-233	27.0 d	7.4 ± 0.1	80.0 ± 1.5	311.9 (0.337)
U	U-238	99.27	Np-239	2.35 d	2.70 ± 0.02	274.6 ± 1.7	277.6 (0.141)
W	W-186	28.4	W-187	23.9 h	37.8 ± 1.5	415 ± 18	479.5 (0.234), 685.7 (0.292)
Yb	Yb-174	31.84	Yb-175	4.19 d	65 ± 5	6.4 ± 4.7	282.6 (0.029), 396.1 (0.062)

Table 3-a

Results of Monostandard NAA of the Granite Rock Samples* (first group), all Element Contents in ppm (μg/gm) Except Fe, K and Na in (%)

Element	AD-45	AD-46	AD-103	AE-73	AR-101	AR-104	AR-107
As	-	-	3.7	5.5	-	-	15.6
Au	-	-	-	-	-	-	-
Ce	-	-	-	76.3	43.5	56	123.65
Co	-	-	-	4.1	6.1	-	-
Cr	-	-	24.7	-	47.5	20.2	97
Cs	-	-	15.6	-	-	-	-
Eu	-	14.1	-	1.9	3.03	2.55	3.22
Fe	1.14	0.93	1.44	1.97	4.48	4.22	2.95
Hf	56.7	39	10	9.12	6.35	7.81	11.57
K	2.77	2.59	3.72	3.85	-	3.81	1.68
La	-	4.3	1.35	39	23.3	24.9	57.4
Lu	-	1.3	1.36	1.7	0.72	1.4	2.4
Na	5.88	6.25	0.20	3.58	3.73	2.88	4.66
Rb	977	698	2100	187	-	-	-
Sb	-	-	-	2.92	-	-	-
Sc	1.8	1.9	3.7	5.24	11.3	11.9	6.32
Sm	3.2	-	0.76	12.8	8.4	10	20.7
Sn	-	-	13562	-	5743	-	-
Ta	775.4	858	124.7	-	-	-	-
Tb	-	-	-	-	-	2.77	2.1
Th	140	53	10.1	10.5	-	7.25	13.13
U	48.2	32.7	-	15.5	-	14.43	10.81
W	-	-	13.14	-	-	-	-
Yb	-	-	2.4	14.2	6.9	10.3	16.3

* These samples have been supplied by the nuclear material authority, Egypt, where the notation of the samples are followed by them.

Table 3-b

Results of Monostandard NAA of the Granite Rock Samples* (second group), all Element Contents in ppm (μg/gm) Except Fe, K and Na in (%)

Element	AS-2	AS-3	AS-5	AS-9	ANA-61	ANA-63	ANW-52	ANW-54
As	39.14	-	116.3	-	-	-	-	-
Au	-	0.102	0.065	-	-	-	-	-
Ce	88.76	90.5	98.6	64.82	37.31	43.76	-	-
Co	-	-	-	5.4	4.7	5.3	-	-
Cr	-	81	-	33.6	-	45.94	-	-
Cs	-	-	-	-	-	-	-	-
Eu	5.8	5.43	5.4	5.4	2.7	2.45	-	-
Fe	4.64	4.51	4.13	3.54	3.62	3.63	1.05	1.58
Hf	19.11	18.04	17.54	18.14	8.21	9	28.4	23
K	-	-	-	-	-	-	-	-
La	36.55	46.15	38.7	46.4	22.5	22.9	-	-
Lu	4	4	3.7	3.76	1.22	1.5	1.7	2.3
Na	4.98	5.05	3.88	4.90	3.48	3.84	6.01	5.46
Rb	-	-	-	-	-	-	816	597.6
Sb	2.46	0.94	-	1.5	-	-	-	-
Sc	7.1	6.76	6.46	4.4	9.61	10.23	1.15	-
Sm	24.6	24.9	24.75	26.1	8.9	10.05	-	-
Sn	1293	2437	2569	3098	-	-	-	-
Ta	-	-	-	4.93	12.6	8.6	299	300
Tb	3	6.11	6.5	7	-	-	-	-
Th	3.7	5.26	9.6	11	8.4	7.9	36.3	38.7
U	-	-	-	-	-	-	25.34	19
W	-	-	-	-	-	-	-	-
Yb	28.13	28.8	26.82	28.7	10.5	10.3	11.75	18.1

* These samples have been supplied by the nuclear material authority, Egypt, where the notation of the samples are followed by them.

Table 4

Data Analysis of Different Granite Ore Samples, ppm, except Na and K in % (group 1)

Element	AD-33	AD-49	AD-101	AE-70	AE-72	AE-74	AR-100	AR-103	AR-105
Ag	-	-	-	-	-	262	-	-	396
As	140	-	-	-	-	6	2	-	209
Au	0.29	-	-	-	-	-	-	-	0.123
Ba	-	-	-	-	-	-	-	-	-
Co	-	-	-	-	-	-	-	-	155
Ga	293.5	1091	1105	312	391	452	306	1025	790
Hf	305	-	-	-	-	-	-	-	70
K	6.8	12	10.6	9.4	9	6.4	10.1	-	-
La	100	-	-	100	87	69	58	42	96
Na	35.8	46	45.4	32	29.4	41	39	36.6	30.8
Sb	-	-	-	-	-	-	-	-	4
Sc	-	-	-	-	-	-	-	-	-
Sm	28.6	-	-	13	15	5	15	6	32
Sn	3450	-	-	-	-	-	12571	6083	4386
Ta	-	442	294	-	-	-	-	-	-
Tb	-	-	-	-	-	-	-	-	-
Th	-	-	-	-	-	-	-	-	18
W	18	15	17	10	15	-	22	-	16
U	6.7	-	17	-	-	6	-	11	9
Zr	1093	-	-	-	-	-	-	-	-

* These samples have been supplied by the Nuclear Material Authority, Egypt, where the notation of the samples are followed by them.

Table 5

Data Analysis of Different Granite Ore Samples, ppm, Except Na and K in % (group 2)

Element	AS-1	AS-8	ANA-60	ANA-62	ANA-64	ANW-51	ANW-53	ANW-55
Ag	101	-	-	-	-	-	-	-
As	152	-	-	-	-	-	-	-
Au	0.31	-	-	-	-	-	-	-
Ba	1104	-	-	-	-	-	-	-
Co	220	-	-	225	-	-	-	-
Ga	-	756	938	608	754	451	726	683
Hf	-	-	-	-	-	-	-	-
K	-	-	-	-	-	-	11	-
La	103	64	-	59	70	-	-	-
Na	39	62.6	38.7	33	30.7	25	45.7	45
Sb	3	2.7	-	-	-	0.92	-	-
Sc	1147	-	-	1829	-	-	-	-
Sm	33	28	12	13	7	0.5	3	-
Sn	3571	-	7244	6825	6350	3832	-	-
Ta	-	-	-	-	-	101	362	334
Tb	8.4	-	-	-	-	-	-	-
Th	7	-	-	-	-	35	53	63
W	-	-	-	-	-	-	-	-
U	7.6	12.7	9.7	6.6	-	7.5	10.7	11.1
Zr	-	-	-	-	-	-	-	-

* These samples have been supplied by the Nuclear Material Authority, Egypt, where the notation of the samples are followed by them.

Table 6

Maximum sensitivity values for the energy range from 0 to 1.5 MeV of natural elements

$(I\sigma/A)_{max}$	Element
> 1000	B, Gd, Sm, Cd
100 - 1000	Eu
10 - 100	Dy, Hg, In, Er, Cl, Hf, H, Lu, Rh, Ir, Sc, Ag, Co, Ho, Ti
1 - 10	Tm, Au, Ta, Se, N(n,p), Re, Ni, Cr, Yb, Ce, Cu, V, K, As, Na, Pt, Mn, Cs, Mo, I, W, La, Br, S
0.1 - 1	Ga, Tb, Pd, Ca, Pr, OS, Fe, Te, Nb, Sr, Y, Ru, Zn, Sb, P, Li, Ce, Mg, Ba, Si, N, Rb
0.01 - 0.1	Zr, Sn, Al, Tl, Be, F
0.001 - 0.01	C, Bi
0.001	Pb, 0

Table 7

Maximum sensitivity values for the energy range from 3 to 10 MeV of natural elements

$(I\sigma/A)_{max}$	Element
328	Gd
10 - 100	Cd, Hg, Dy, Cl
1 - 10	Ti, Co, Sc, Ir, Ni, Mn, Au, Rh, Nd, Cu, V, Cr, Hf, Fe, Yb, Y
0.1 - 1	Ag, S, Se, Na, Ga, Si, La, W, K, Cs, Ca, Pt, Pr, Zn, As, Al, Ba, N, Te, P, Mg
0.01 - 0.1	Br, Mo, I, Ce, Pd, Pb, Sr, Ge, Tl, Sb, Zr, Ru, C, Rb, Nb
0.01	Li, F, Bi
Elements with $I_\sigma < 1$ %	In, Sn, Sm, Eu, Tb, Ho, Er, Tm, Lu, Ta, Re, OS

Table 8

Capture γ-ray sensitivity for elements of interest in ore samples

Element	Cross-Section (barns)	Atomic Mass (A)	Energy (keV)	Intensity (I)	Sensitivity ($I\sigma/A$)
Gd	39100	157.25	247	22.18	5515.0
			1185	5.93	1475.0
Mn	13.3	54.938	847	15.56	3.77
			1810	35.80	8.67
SM	5840	150.35	334	83.26	3234.0
			439	45.79	1779.0

Table 9

Comparison between the data obtained by PGNAA using the available facility and those found by RNAA. Average error: 25 %

Sample	Element	Net Coun./gm/ 100 min x 10^{-1}	Conc. (µg/gm) present work	Conc. (µg/gm) RNAA	Error %
Monazite	Sm	2150 ± 350	200	150	33
	Gd	754 ± 150	115	92	25
	Mn	356 ± 70	1800	2270	21
Phosphate	Sm	-	-	65	-
	Gd	-	-	-	-
	Mn	700 ± 150	3350	4200	20

Figure Captions

Fig. 1 Detector efficiency curve at geometry 10 cm

Fig. 2 Detector efficiency curve at geometry 40 cm

Fig. 3 Gamma-ray spectrum of granite (AD-103 from group 1) rock sample. 5 d decay time, 50 min counting time, sample-weight 127 mg

Fig. 4 Gamma-ray spectrum of granite (AD-103 from group 1) rock sample. 22 d decay time, 50 min counting time, sample-weight 127 mg

Fig. 5 Gamma-ray spectrum of granite (AS-3 from group 2) rock sample. 6 d decay time, 50 min counting time, sample-weight 122 mg

Fig. 6 Gamma-ray spectrum of granite (AS-3 from group 2) rock sample. 21 d decay time, 50 min counting time, sample-weight 122 mg

Fig. 7 X-ray analysis of granite ore sample AD-101

Fig. 8 X-ray analysis of granite ore sample AE-70

Fig. 9 X-ray analysis of granite ore sample AR-100

Fig. 10 X-ray analysis of granite ore sample AS-1

Fig. 11 X-ray analysis of granite ore sample ANA-60

Fig. 12 X-ray analysis of granite ore sample ANW-51

Fig. 13 Gamma-ray spectrum of epithermal neutron irradiation of Ad-33 granite rock sample. Cooling time: 2 d, sample-weight: 174 mg

Fig. 14 Gamma-ray spectrum of epithermal neutron irradiation of AR-105 granite rock sample. Cooling time: 4 d, sample-weight: 121 mg

Fig. 15 Gamma-ray spectrum of epithermal neutron irradiation of AS-1 granite rock sample. Cooling time: 6 d, sample-weight: 157 mg

Fig. 16 Sketch of experimental arrangement of PGNAA facility showing the relative positions of the Ge(Li) detector, shield, Cf^{252} neutron source and the sample

Fig. 17 Calibration curve for samerium determination using the gamma-ray lines at 334 keV and 439 keV

Fig. 18 Calibration curve for gadolinium determination using the gamma-ray line at 1185 keV

Fig. 19 Calibration curve for manganese determination using the gamma-ray lines at 847 keV and 1810 keV

Fig. 20 Neutron-capture gamma-ray spectrum of monazite sand using Cf^{252} neutron source. Measuring time: 17 h, sample-weight: 22.6 gm

Fig. 21 Neutron-capture gamma-ray spectrum of phosphate ore using Cf^{252} neutron source. Measuring time: 17 h, sample-weight: 20.6 gm

Fig. (1) Detector efficiency curve at geometry 10 cm

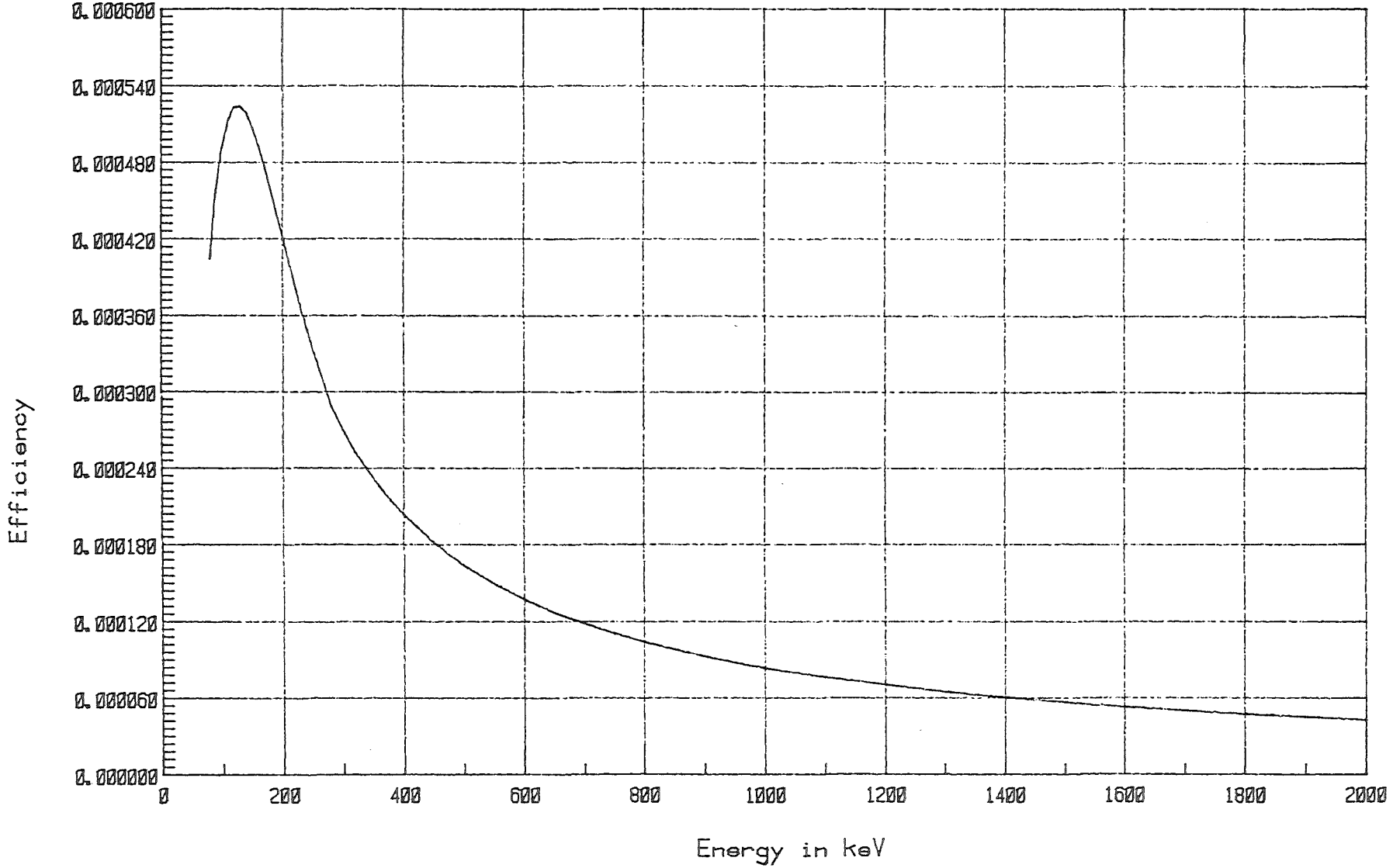

Fig. (2) Detector efficiency curve at geometry 40 cm

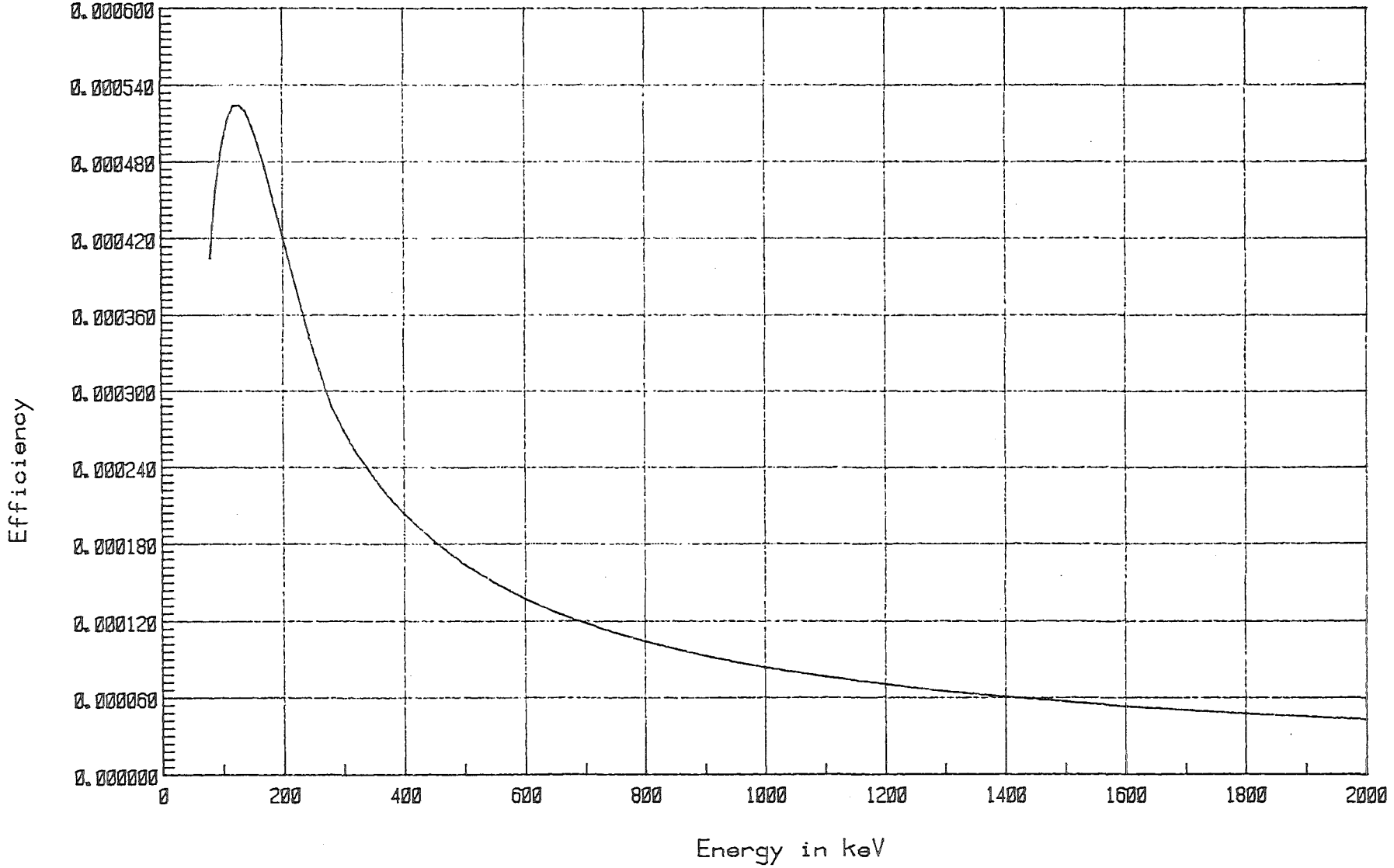

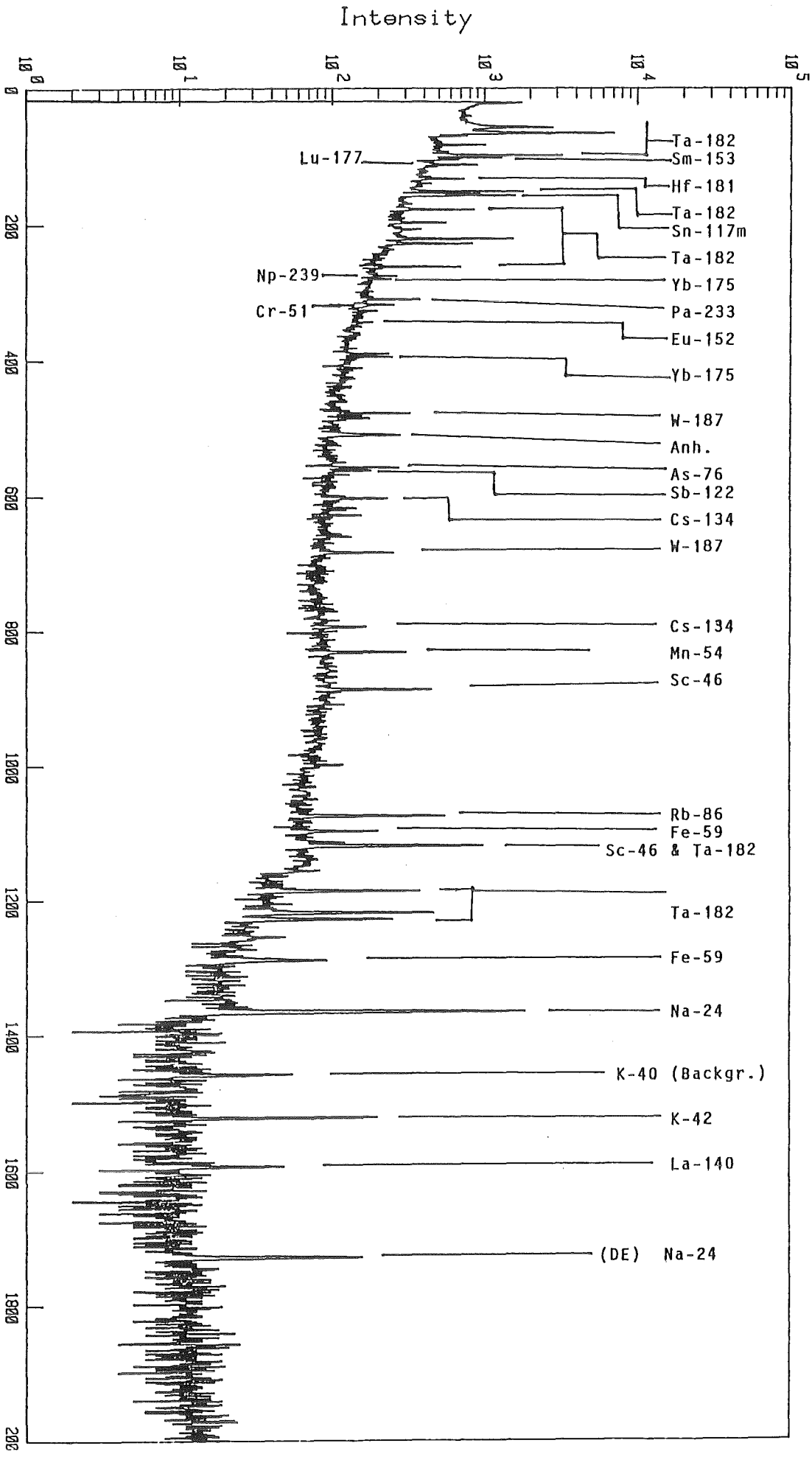

Fig. (3) : Gamma-Ray Spectrum of Granite (AD-103 from Group 1) rock Sample
5 d. Decay Time, 50 min. Count. Time, Sample-Weight 127 mg

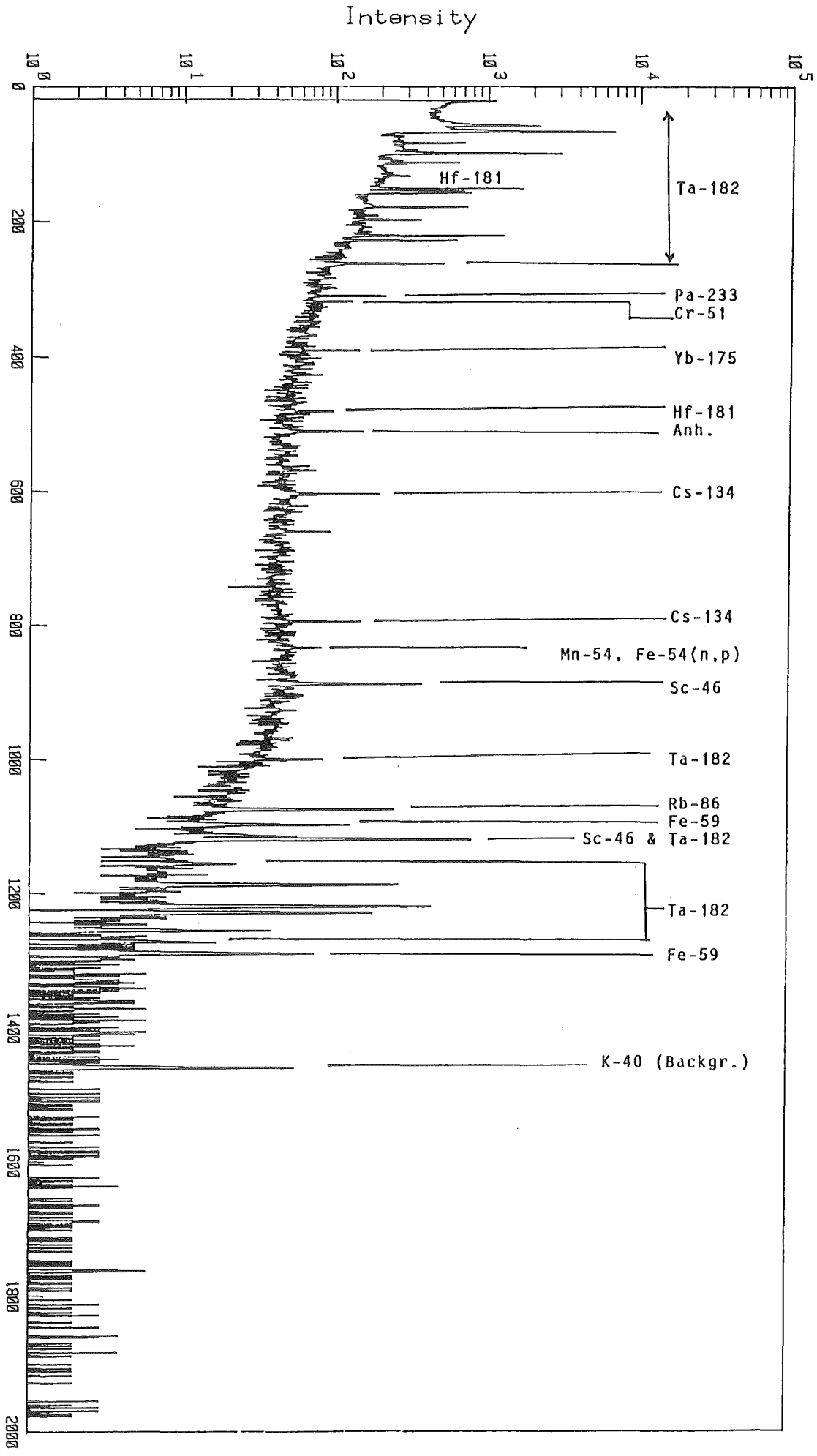

Fig. (4) : Gamma-Ray Spectrum of Granite (AD-103 from Group 1) rock Sample
22 d. Decay Time, 50 min. Count. Time, Sample-Weight 127 mg

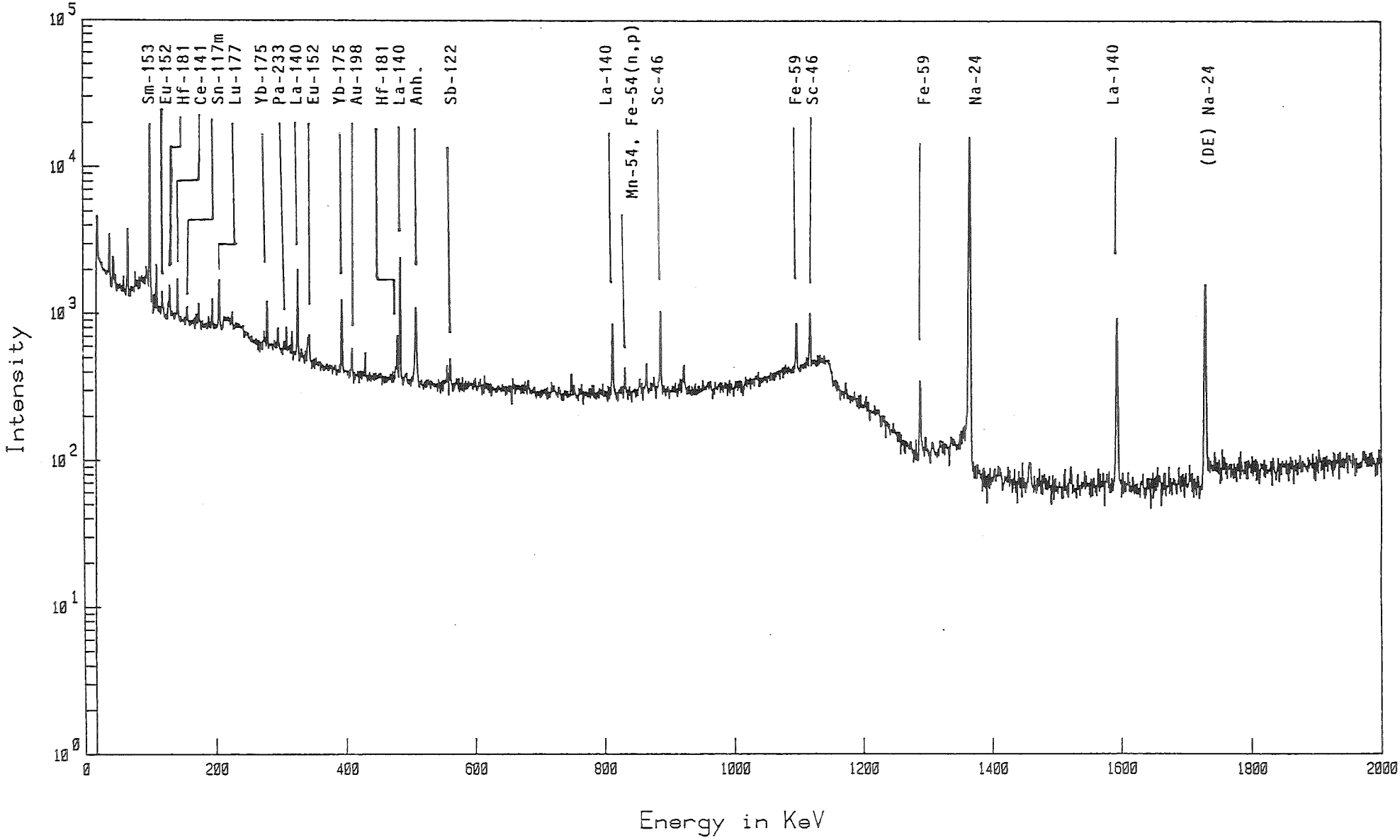

Fig. (5) : Gamma-Ray Spectrum of Granite (AS-3 from Group 2) rock Sample
6 d. Decay Time, 50 min. Count. Time, Sample-Weight 122 mg

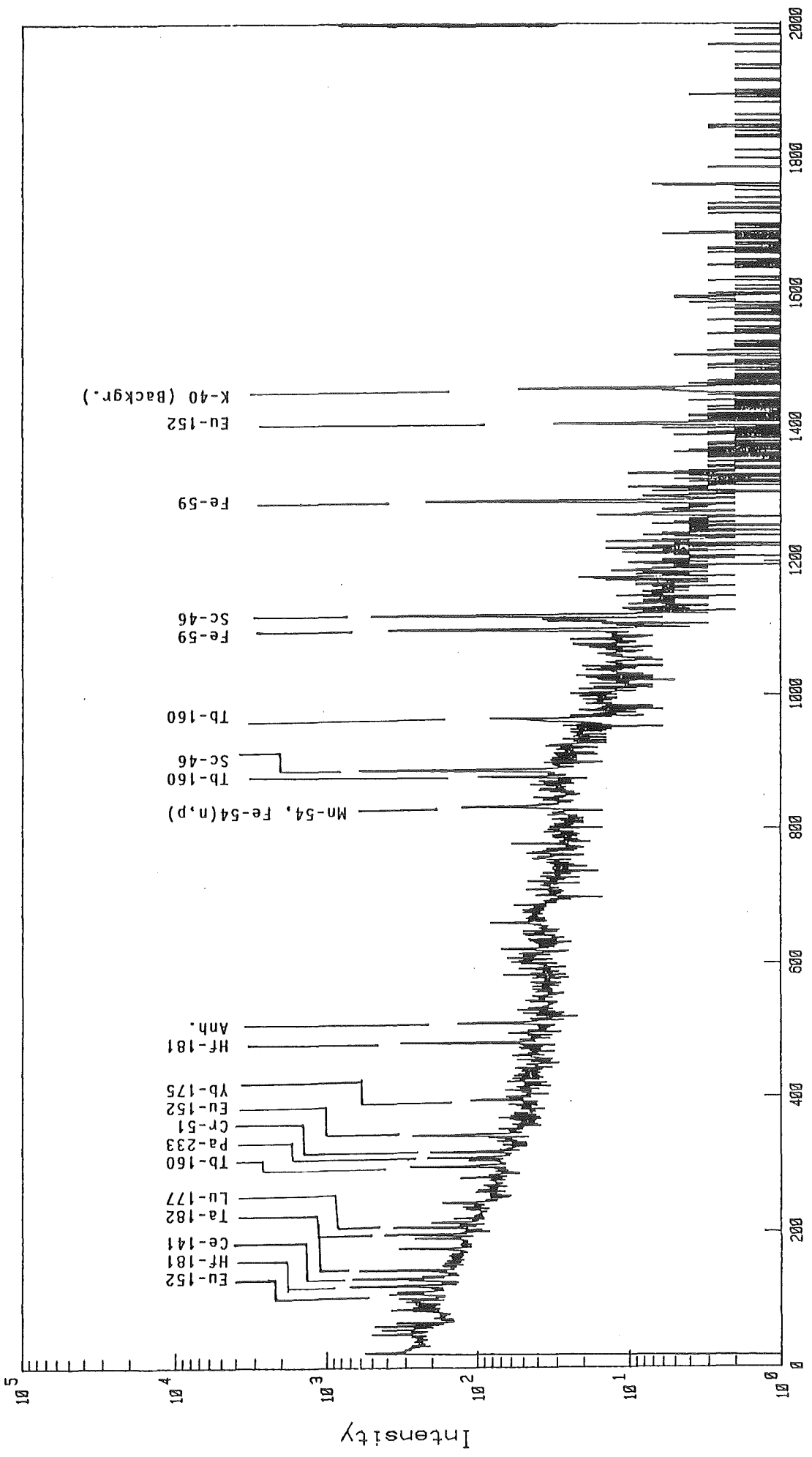

Fig. (6) : Gamma-Ray Spectrum of Granite (AS-3 from Group 2) rock Sample
21 d. Decay Time, 50 min. Count.Time, Sample-Weight 122 mg

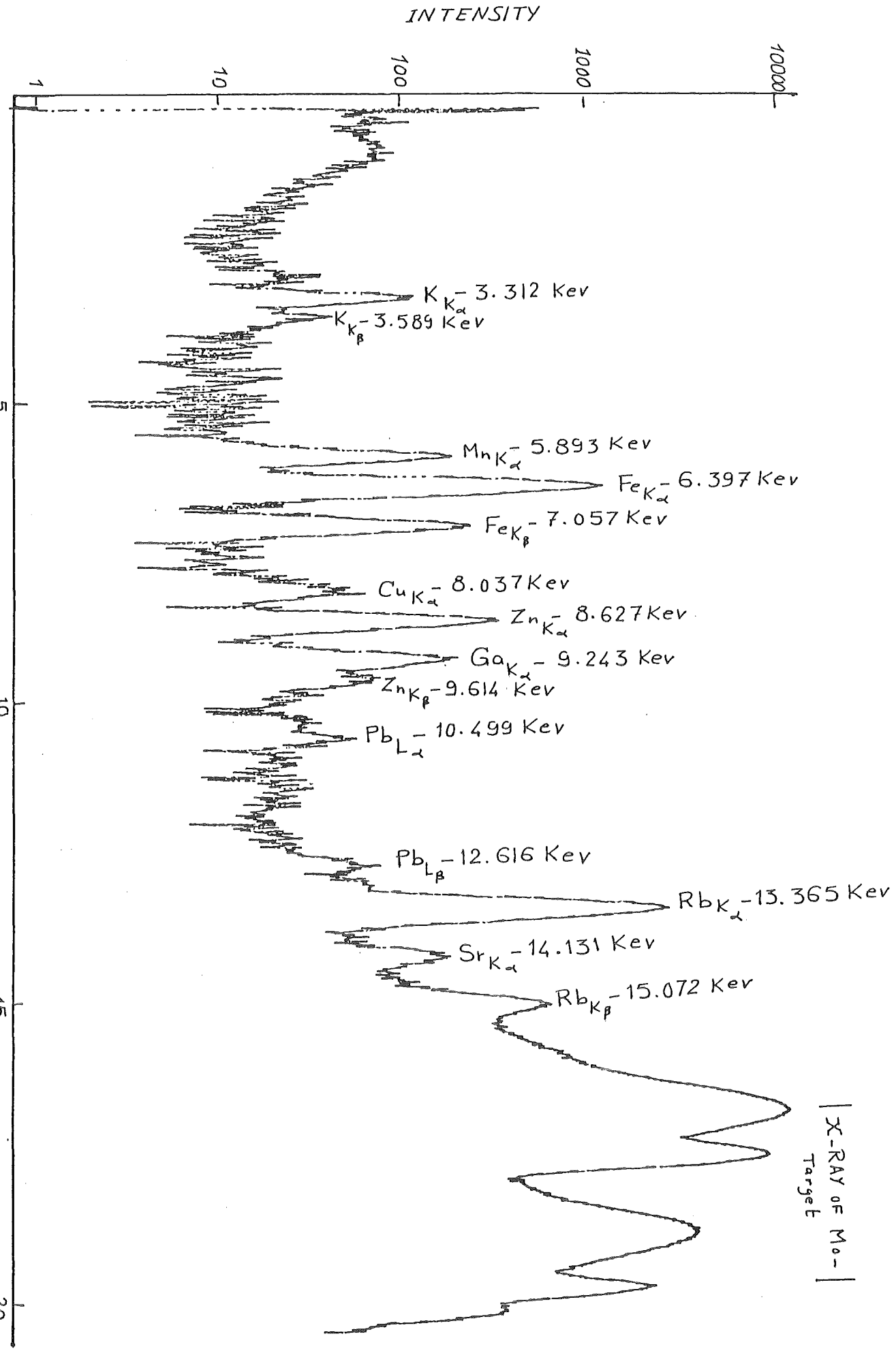

Fig. (7) X-RAY ANALYSIS OF GRANITE ORE SAMPLE-AD 101

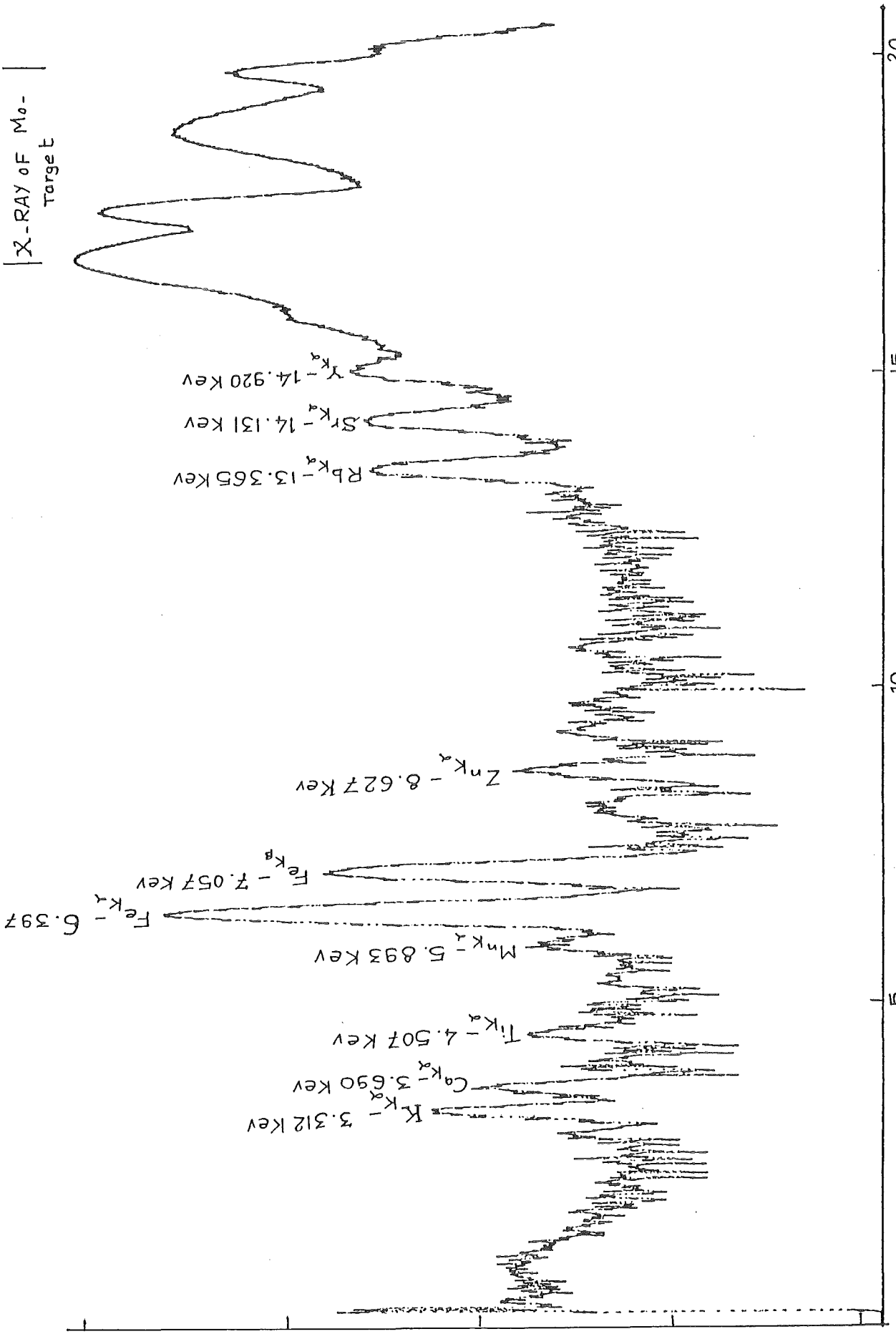

Fig. (8) X-RAY ANALYSIS OF GRANITE ORE SAMPLE-AE 70

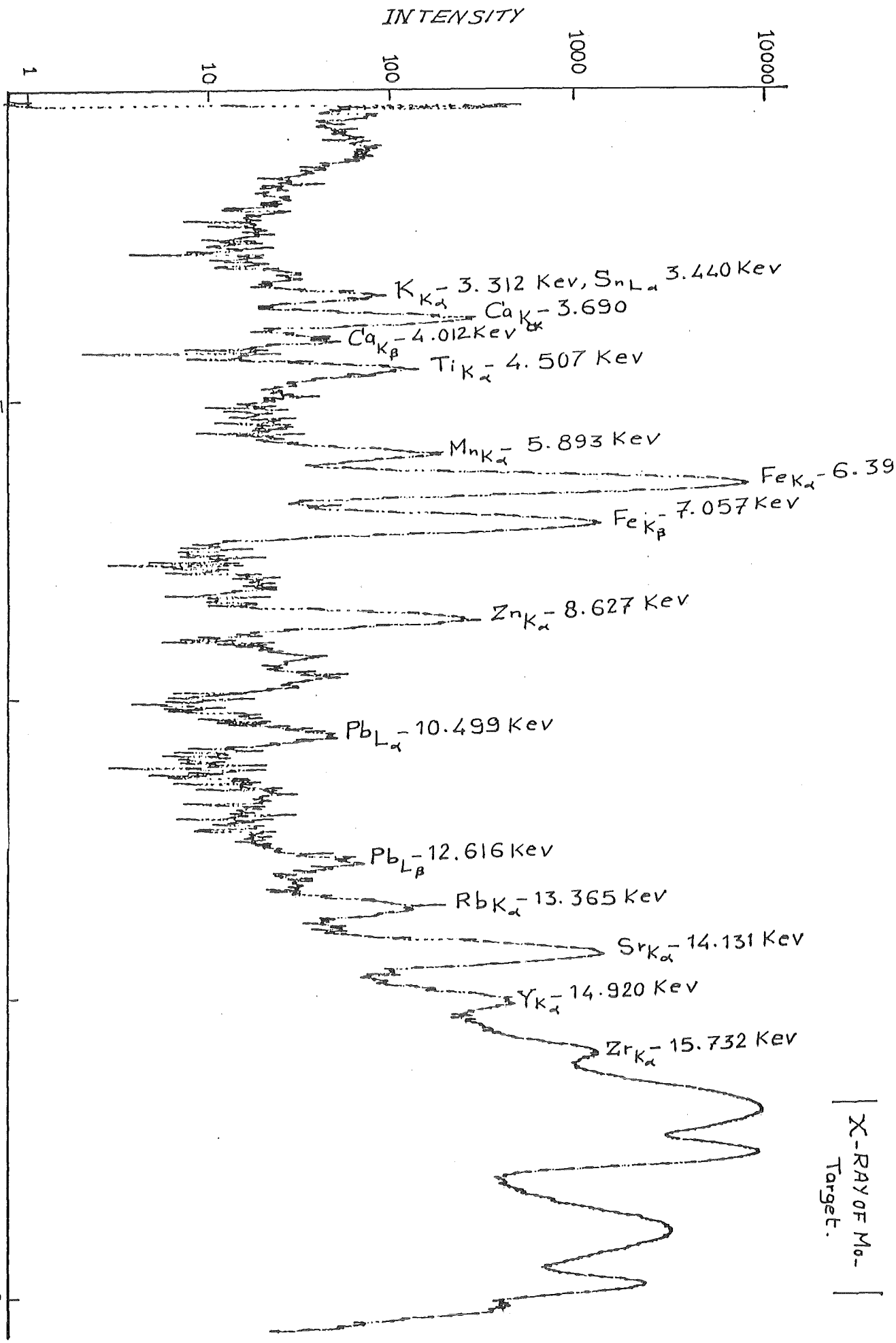

Fig. (9) X-RAY ANALYSIS OF GRANITE ORE SAMPLE - AR 100

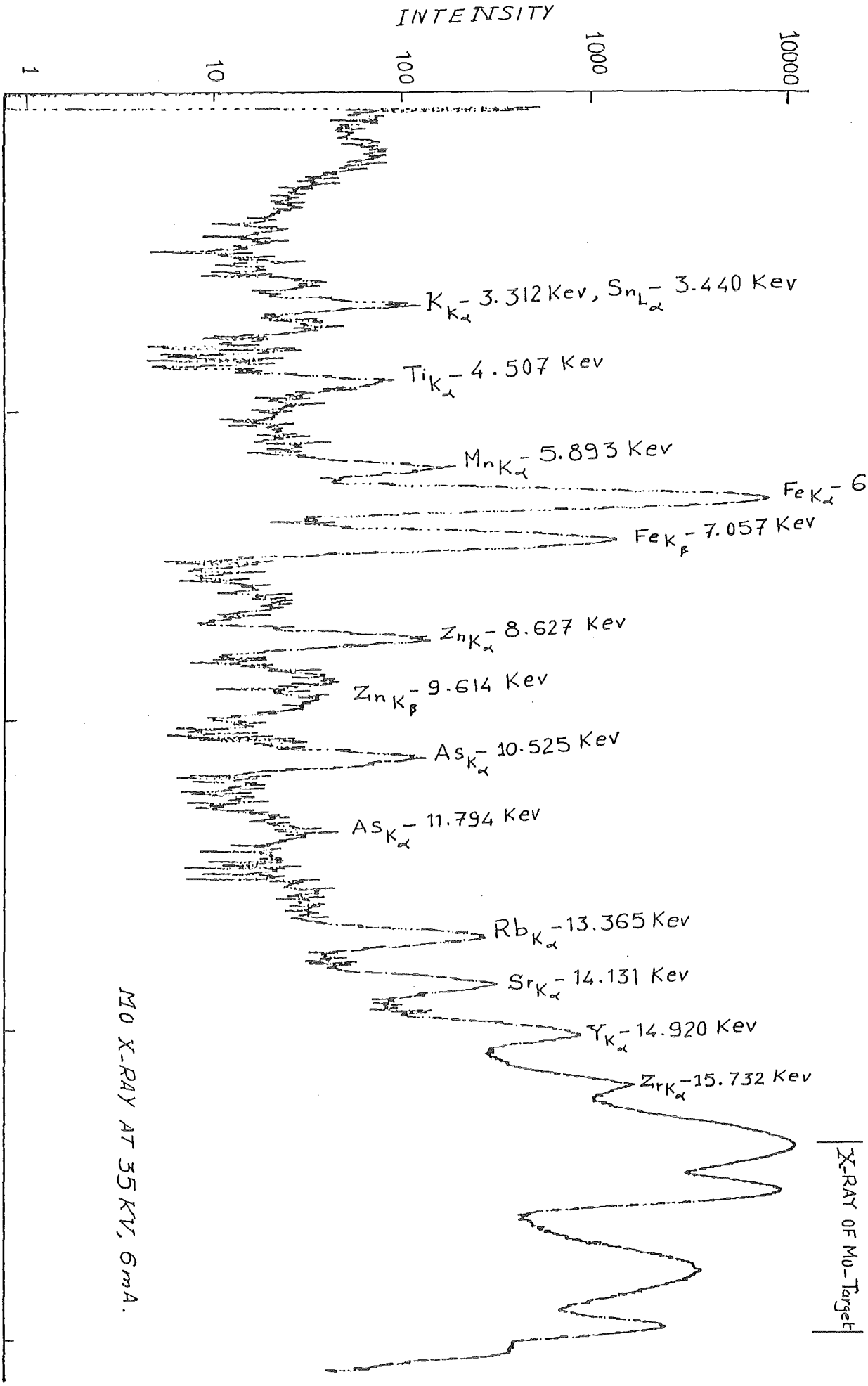

Fig.(10) X-RAY ANALYSIS OF GRANITE ORE SAMPLE-AS1

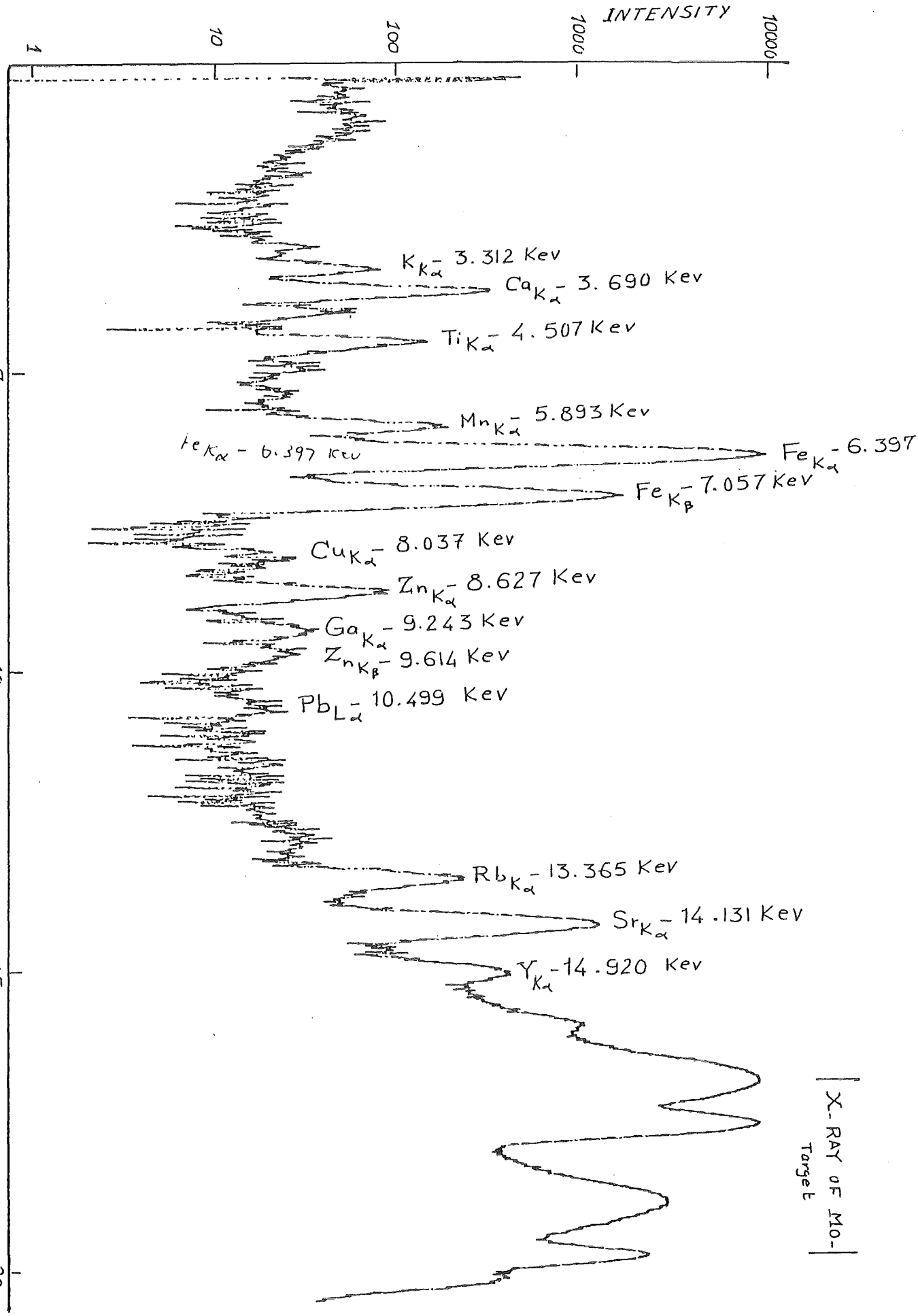

Fig. (11) X-RAY ANALYSIS OF GRANITE ORE SAMPLE-ANA 60

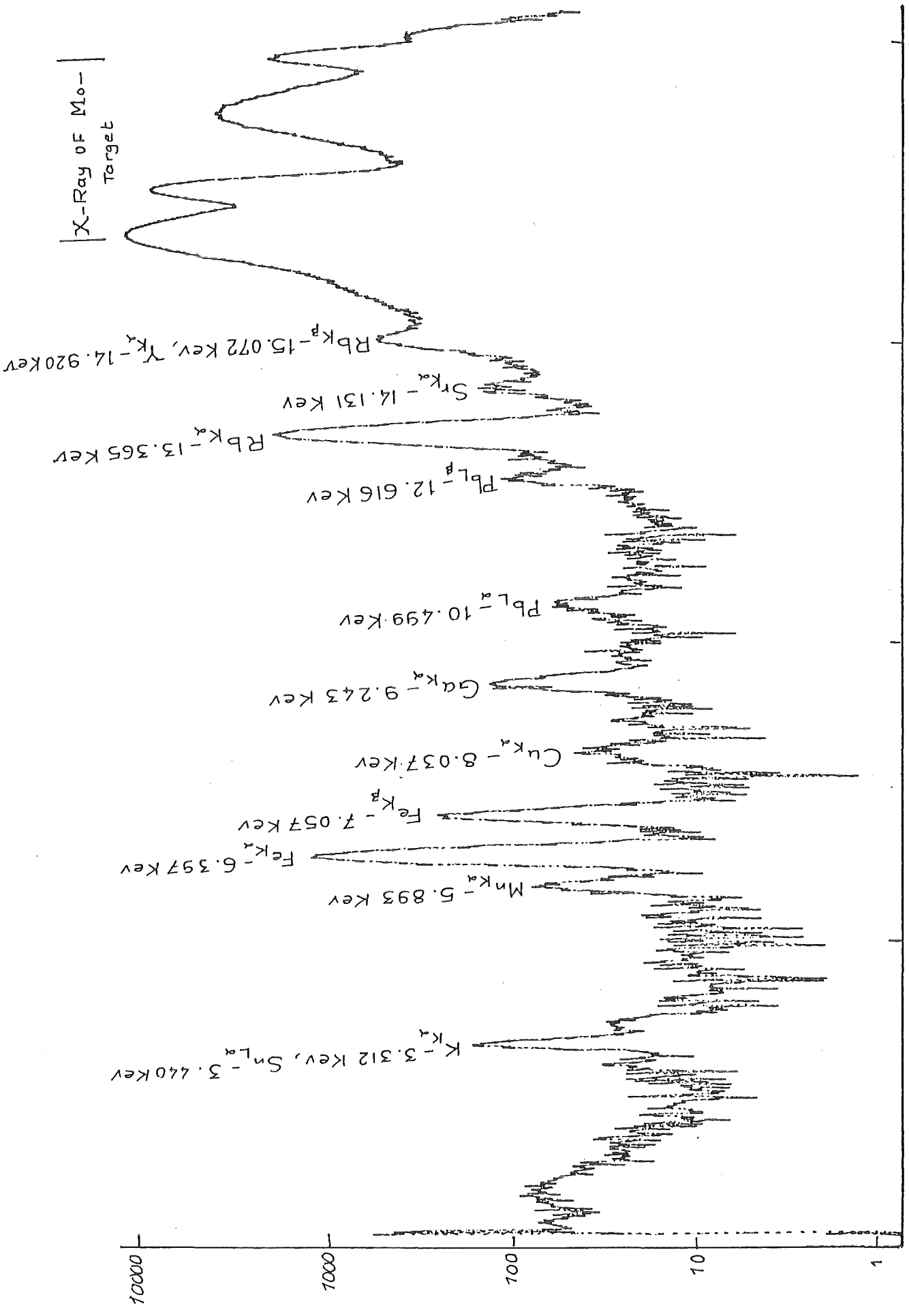

Fig. (12) X-RAY ANALYSIS OF GRANITE ORE SAMPLE_ANW 51

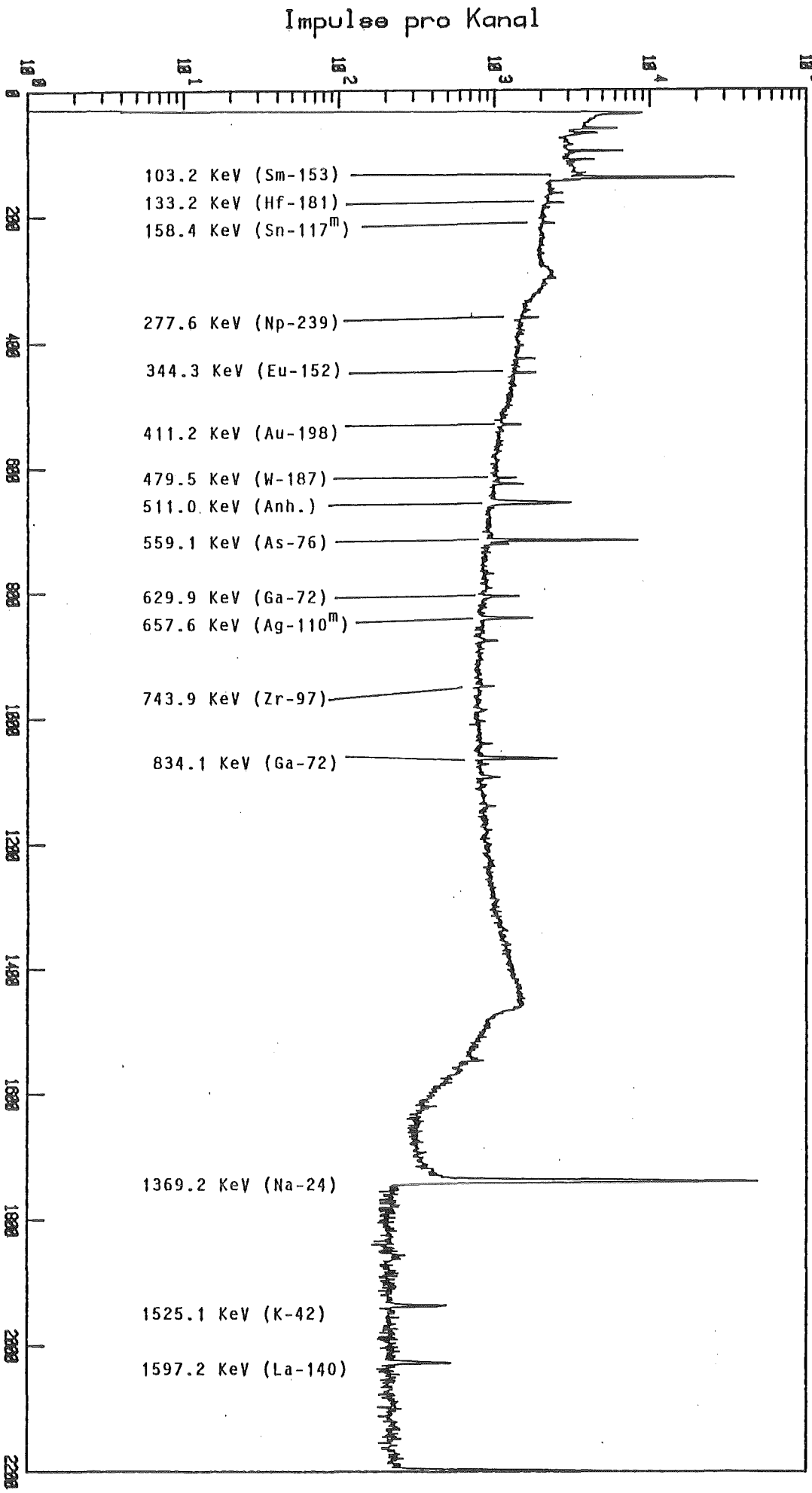

Fig. (13) : Gamma-ray spectrum of epithermal neutron irradiation of AD-33 Granite rock sample.
Cooling time : 2 d. , Sample weight : 174 mg.

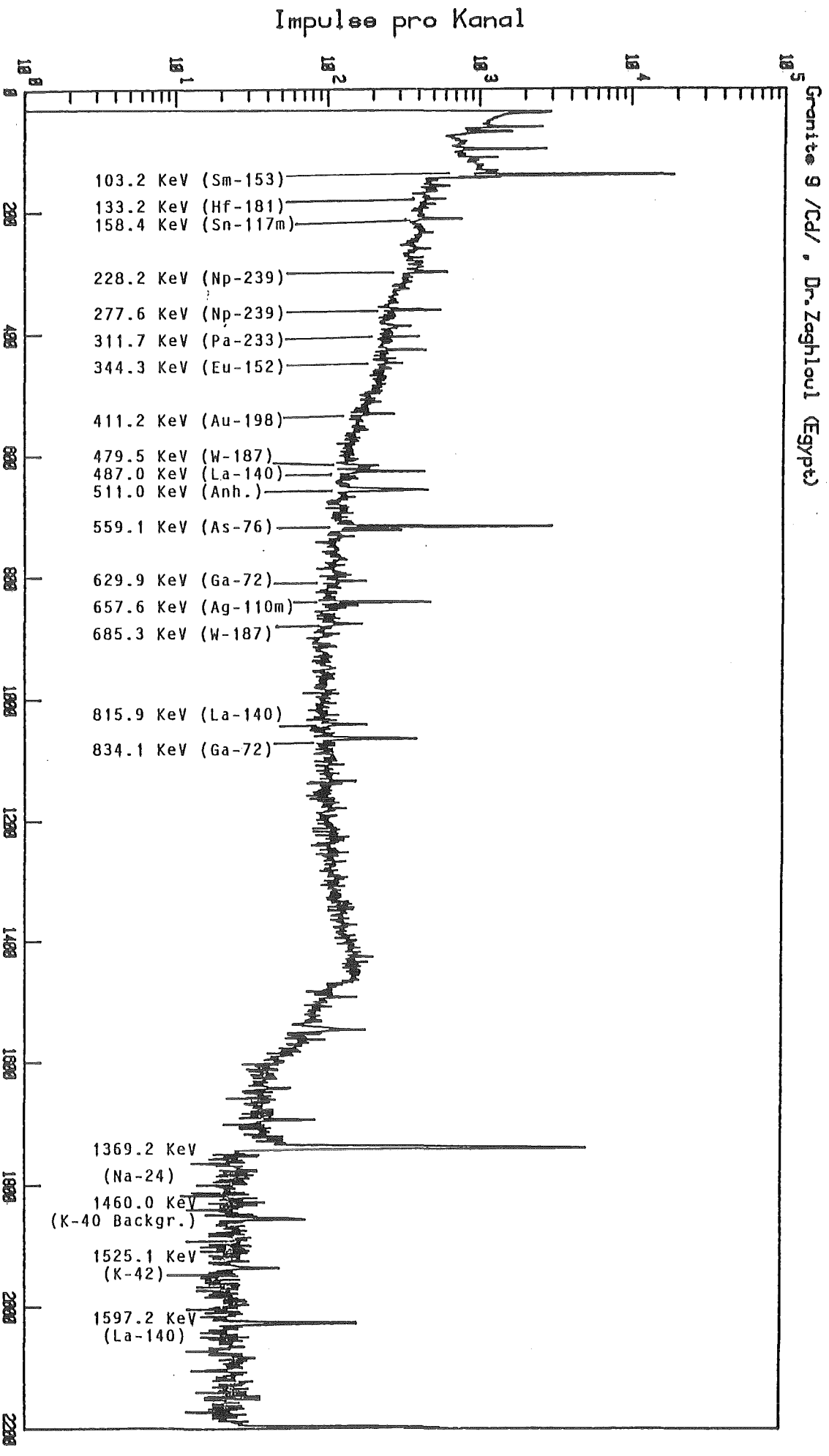

Fig. (14) : Gamma-ray spectrum of epithermal neutron irradiation of AR-105 Granite rock sample.
Cooling time : 4 d. , Sample weight : 121 mg.

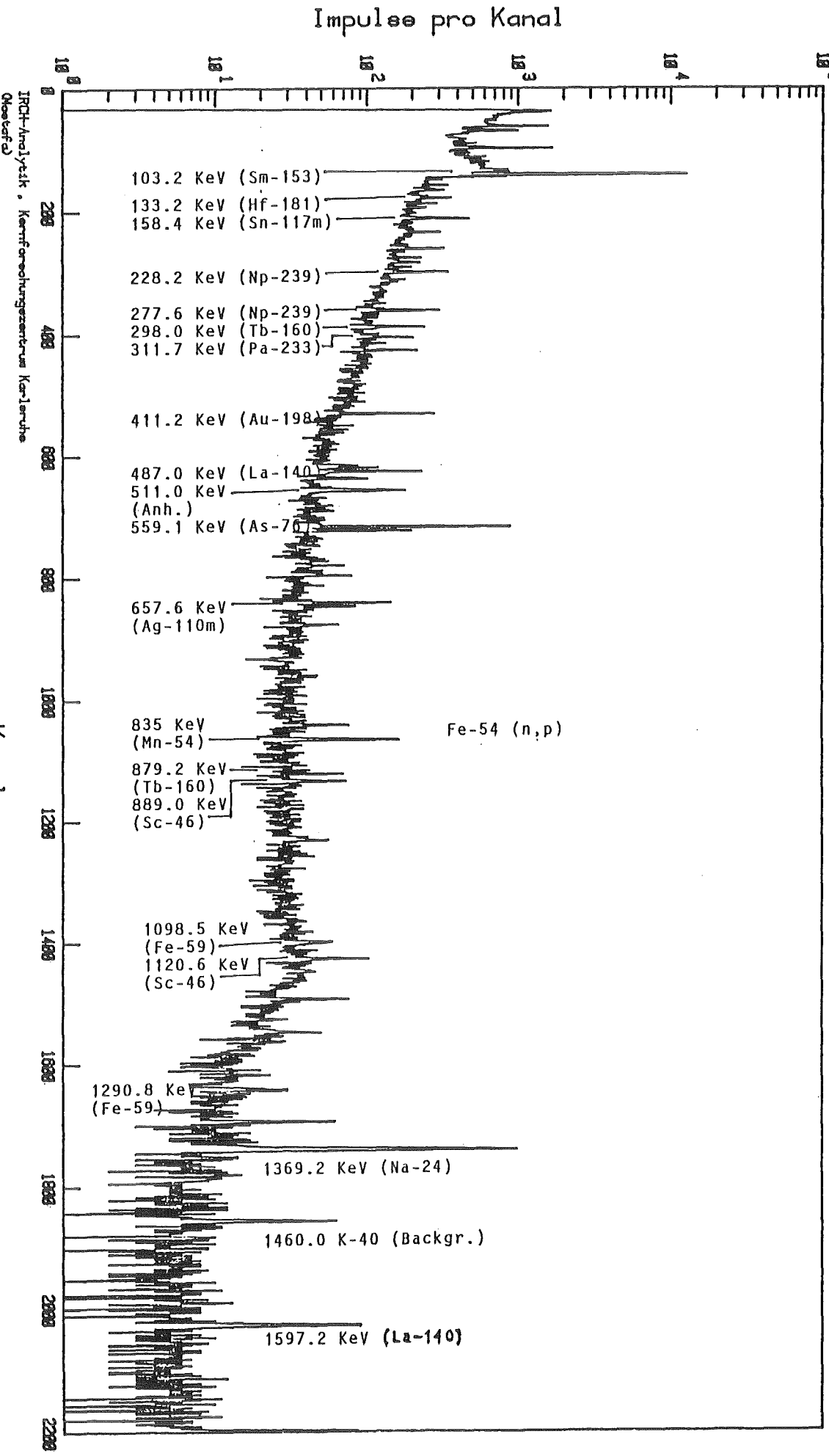

Fig. (15): Gamma-ray spectrum of epithermal neutron irradiation of AS-1 Granite rock sample.
Cooling time : 6 d. , Sample weight : 157 mg.

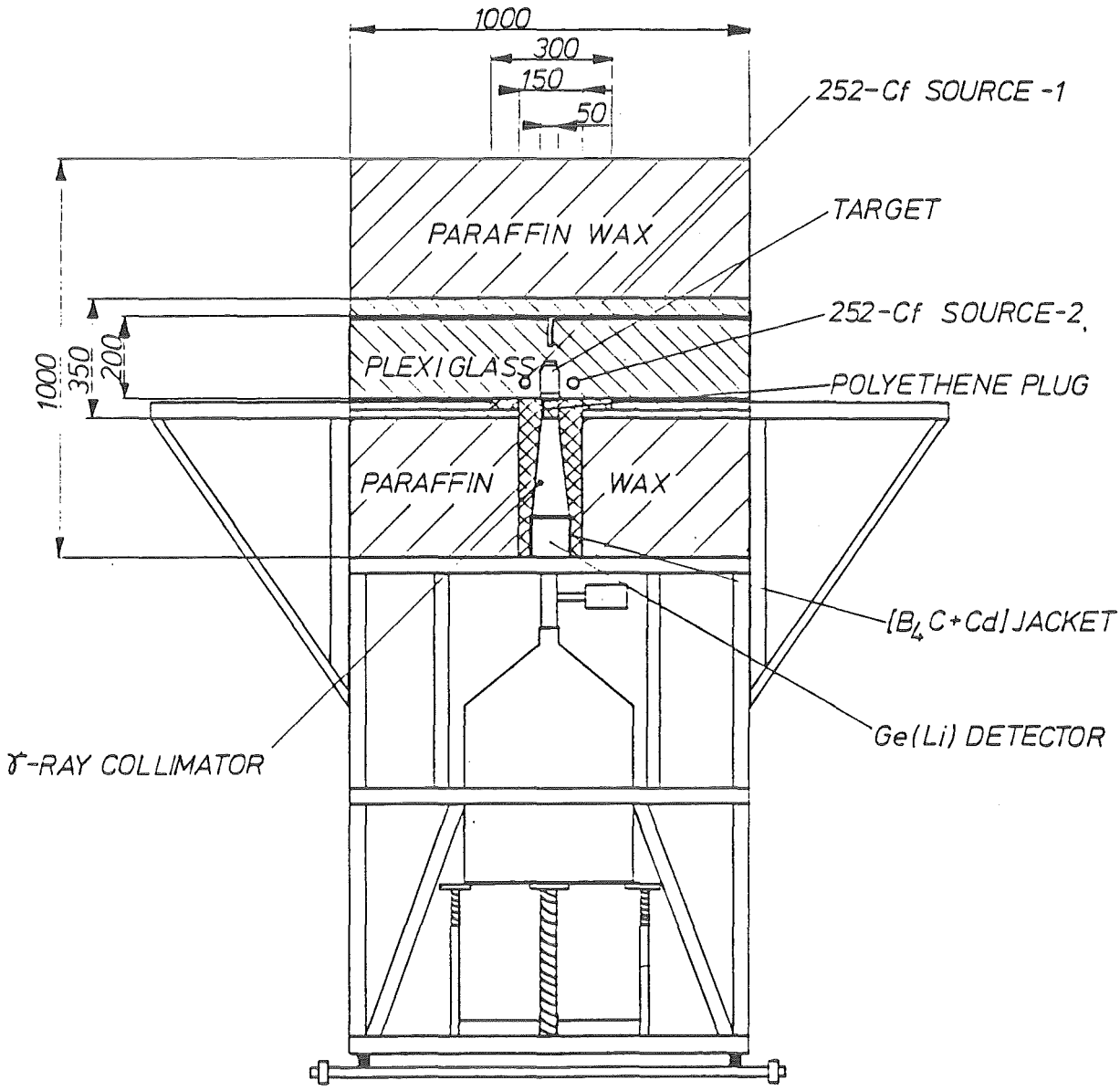

Fig. (16) : Sketch of experimental arrangement of PGNAA facility showing the relative positions of the Ge(Li)-detector, Shield, Cf-252 Neutron Source and the Sample.

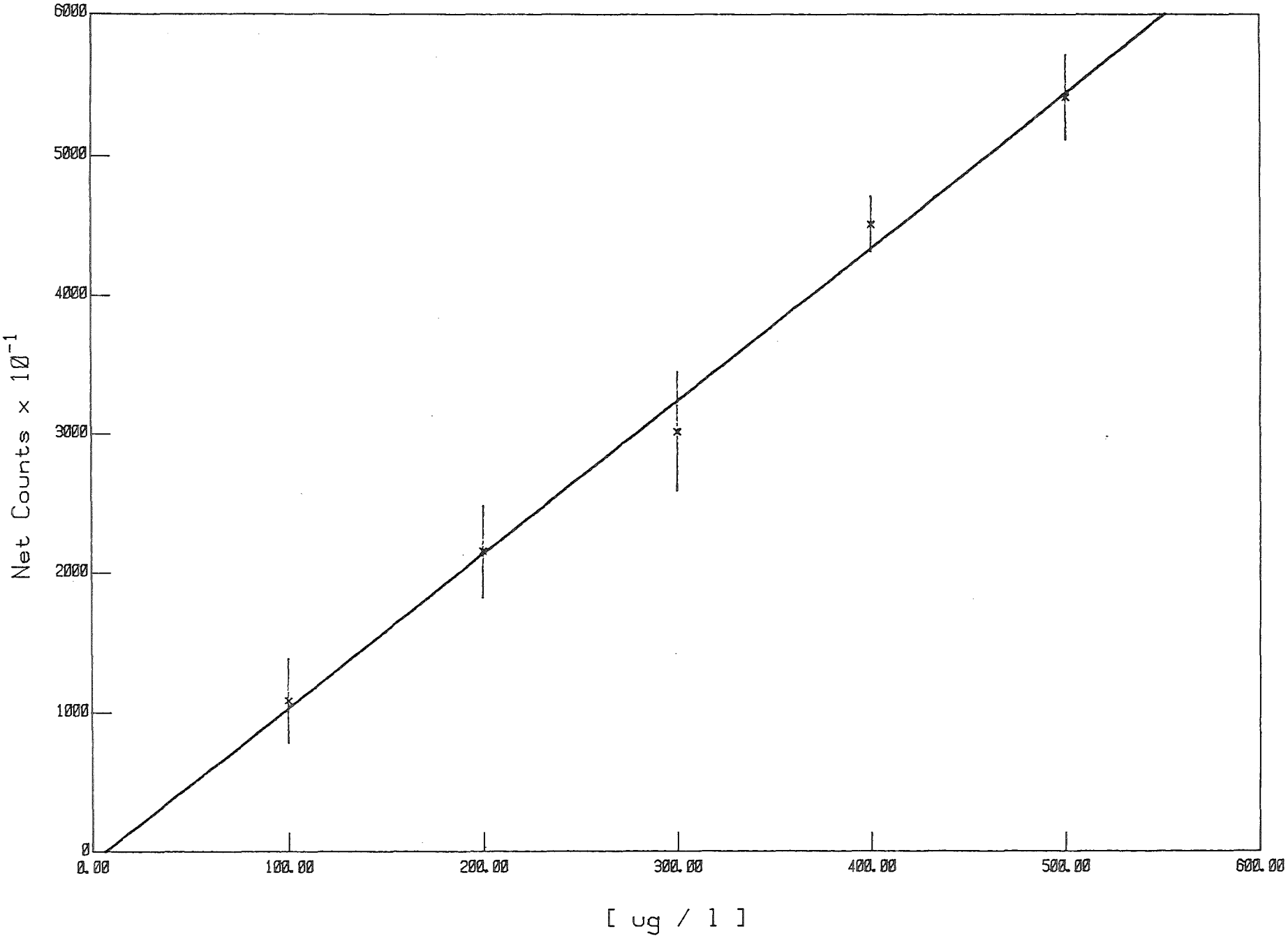

Fig. (17) : Calibration Curve for Samerium determination using the Gamma-ray lines 334.0 KeV and 439.0 KeV

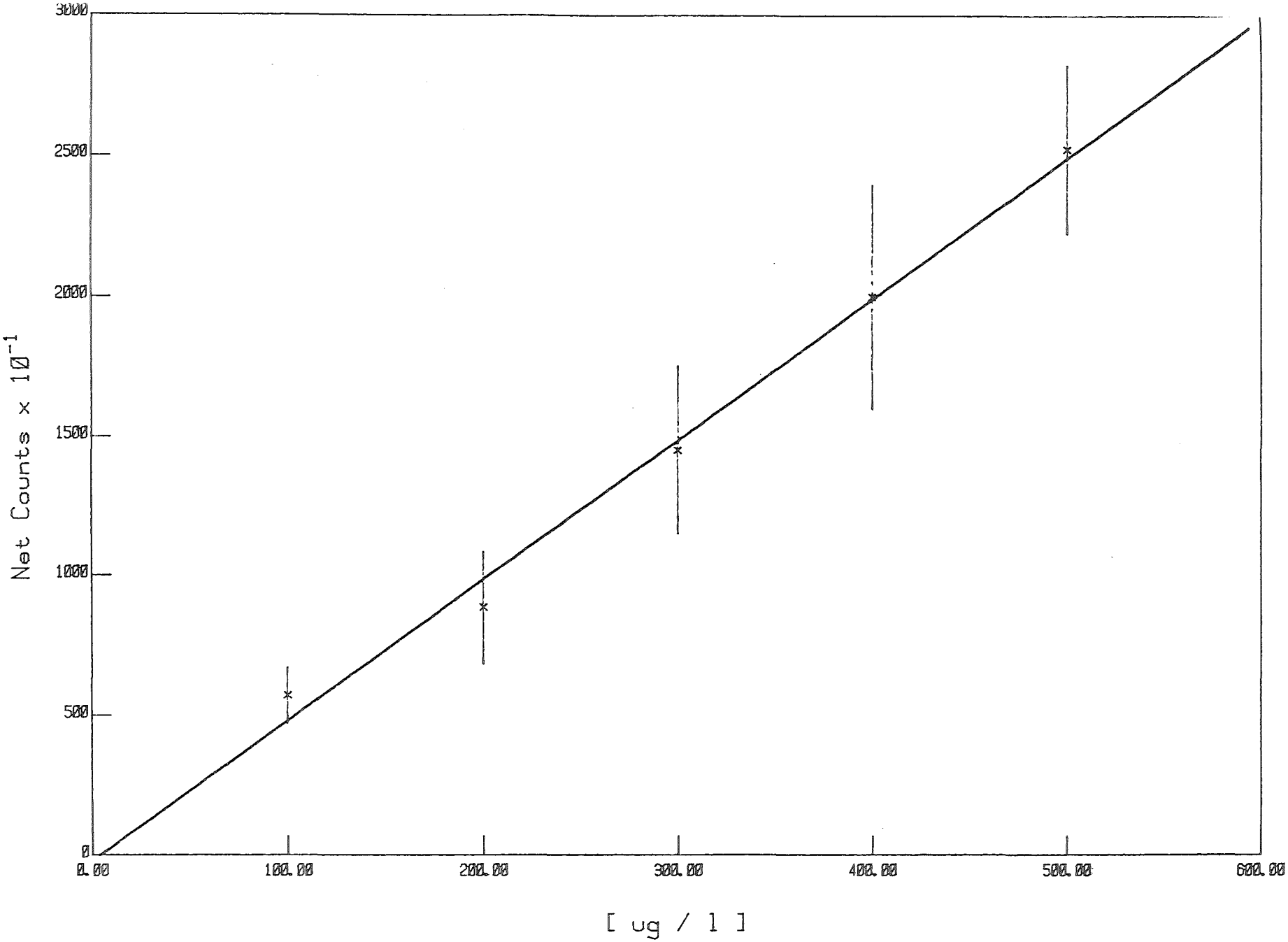

Fig. (18): Calibration Curve for Gadolinium determination using the Gamma-ray line 1185.0 KeV

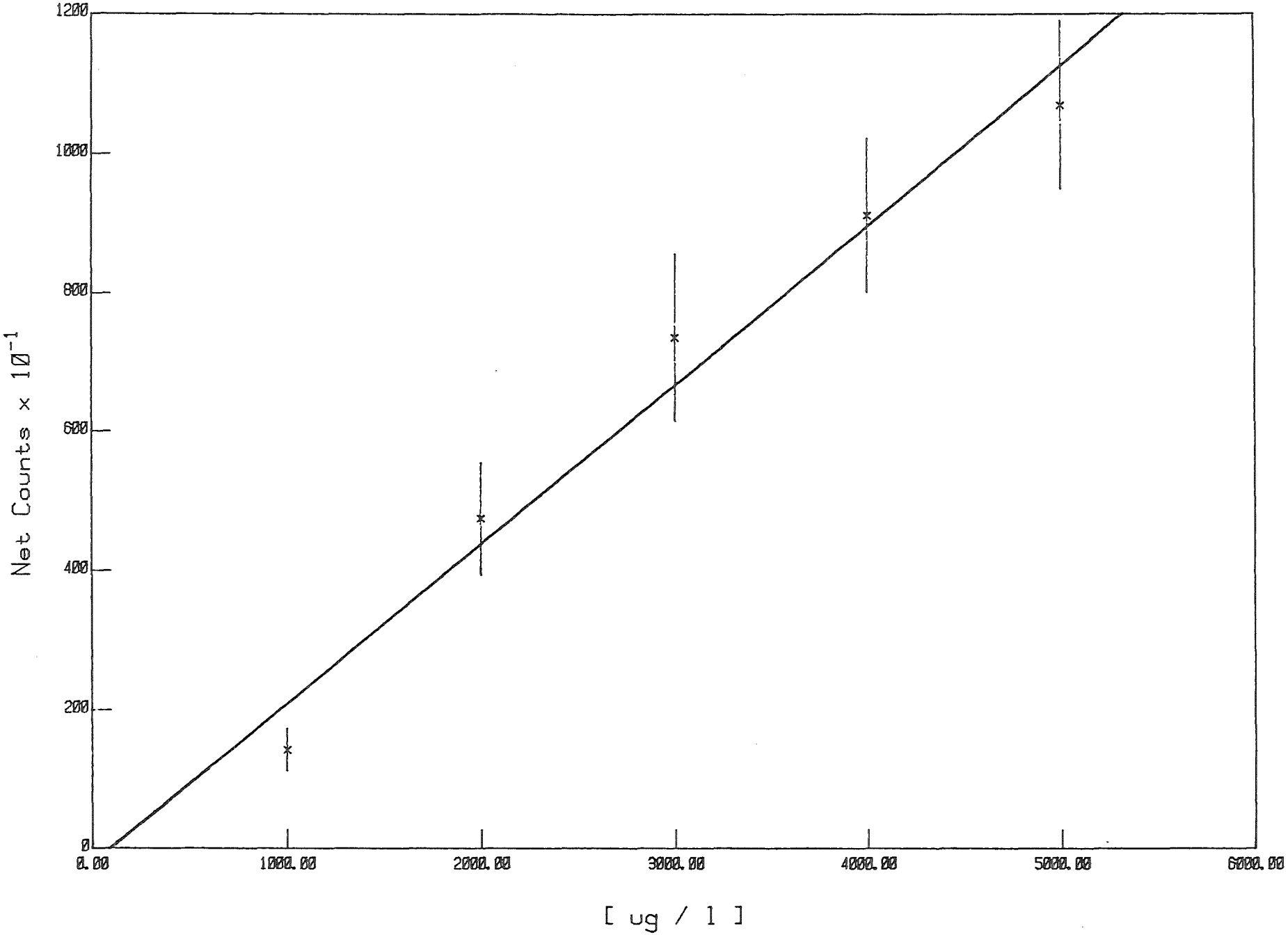

Fig.(19) : Calibration Curve for Manganese determination using the Gamma-ray lines 847.0 KeV and 1810.0 KeV

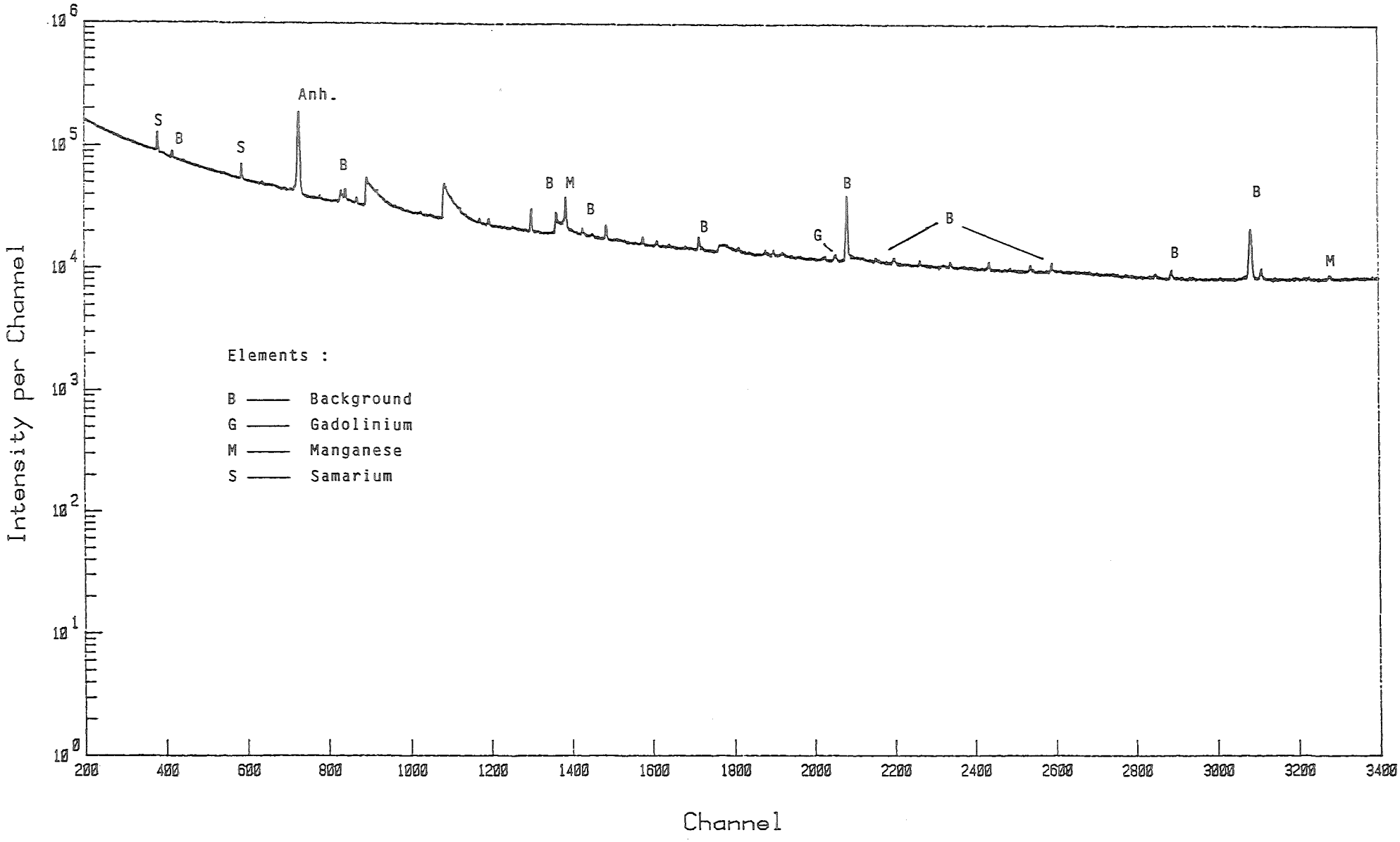

Fig. (20) : Neutron-Capture Gamma-Ray Spectrum of Monazite Sand Using Cf-252 Source. Measuring Time 17 h., Sample-Weight 22.6 gm

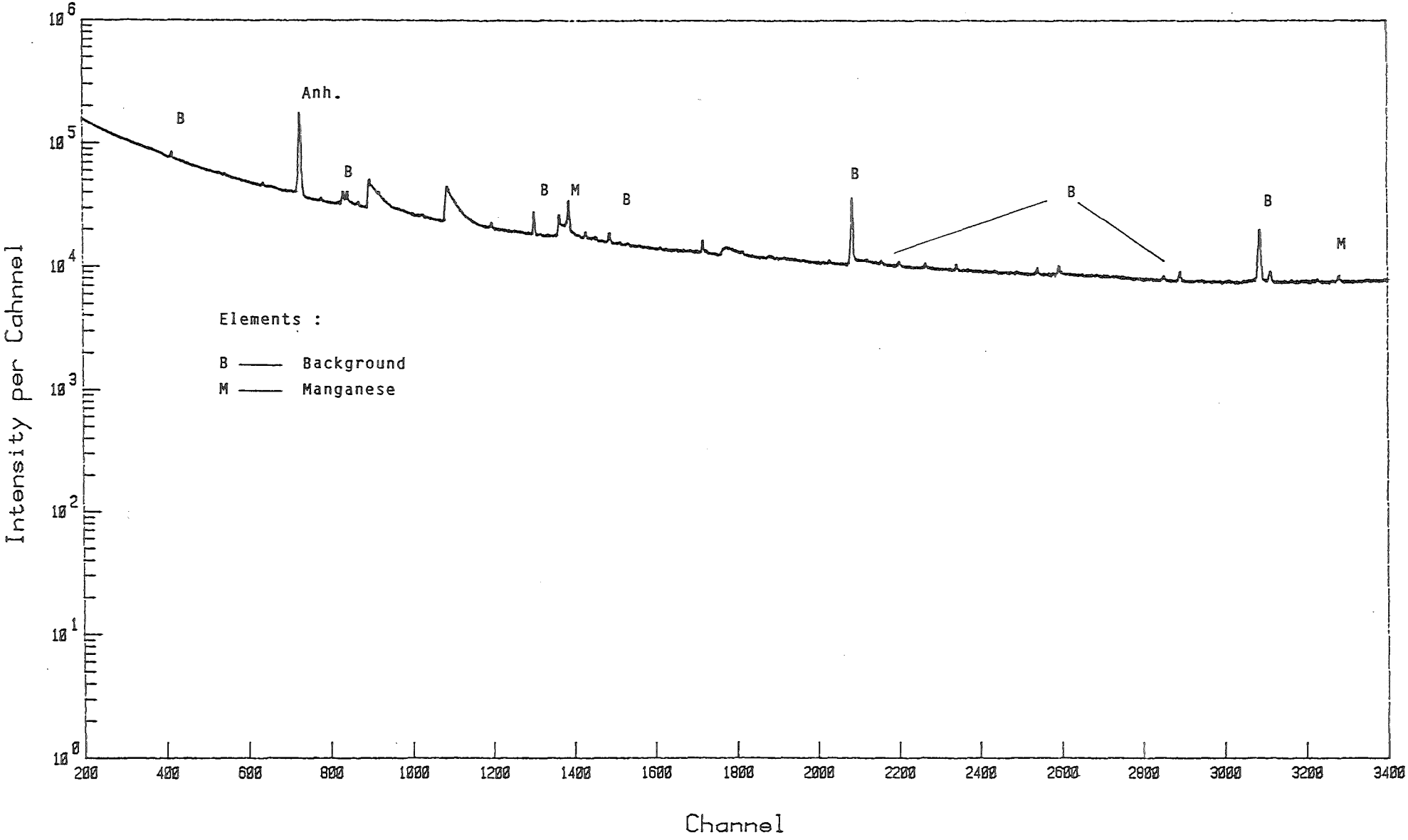

Fig. (21): Neutron-Capture Gamma-Ray Spectrum of Phosphate ore, Uisng Cf-252 Source. Measuring Time 17 h., Sample-Weight 12.4 gm.